DESIGN AND CHARACTERIZATION OF THIN STAINLESS STEEL BURST DISKS FOR INCREASING TWO-STAGE LIGHT GAS LAUNCHER EFFICIENCY

Jonathan M. Tylka*, Kenneth L. Johnson**
Donald Henderson* and Karen Rodriguez******

*NASA Co-operative Student, Department of Mechanical and Aerospace Engineering, University of Missouri, Columbia, Missouri, 65201
**Statistician, NESC, NASA-MSFC, NESC Engineering Office, MS EE04L/NESC, Huntsville, Alabama, 35812;
***Hypervelocity Impact Testing Group Leader, NASA-JSC White Sands Test Facility, RF, 12600 NASA Rd., Las Cruces, New Mexico 88012;
**** Hypervelocity Impact Testing Project Manager, NASA-JSC White Sands Test Facility, RF, 12600 NASA Rd., Las Cruces, New Mexico 88012

Summary—Laser etched 300 series Stainless Steel Burst Disks (SSBD) ranging between 0.178 mm (0.007-in.) and 0.508mm (0.020-in.) thick were designed for use in a 17-caliber two-stage light gas launcher. First, a disk manufacturing method was selected using a combination of wire electrical discharge machining (EDM) to form the blank disks and laser etching to define the pedaling fracture pattern. Second, a replaceable insert was designed to go between the SSDB and the barrel. This insert reduced the stress concentration between the SSBD and the barrel, providing a place for the petals of the SSDB to open, and protecting the rifling on the inside of the barrel. Thereafter, a design of experiments was implemented to test and characterize the burst characteristics of SSBDs. Extensive hydrostatic burst testing of the SSBDs was performed to complete the design of experiments study with one-hundred and seven burst tests. The experiment simultaneously tested the effects of the following: two SSBD material states (full hard, annealed); five SSBD thicknesses 0.178, 0.254, 0.305, 0.381 mm (0.007, 0.010, 0.012, 0.015, 0.020-in.); two grain directions relative); number of times the laser etch pattern was repeated (varies between 5-200 times); two heat sink configurations (with and without heat sink); and, two barrel configurations (with and without insert). These tests resulted in the quantification of the relationship between SSBD thickness, laser etch parameters, and desired burst pressure. Of the factors investigated only thickness and number of laser etches were needed to develop a mathematical relationship predicting hydrostatic burst pressure of disks using the same barrel configuration. The fracture surfaces of two representative SSBD bursts were then investigated with a scanning electron microscope, one burst hydrostatically in a fixture and another dynamically in the launcher. The fracture analysis verified that both burst conditions resulted in a ductile overload failure indicated by transgranular microvoid coalescence, non-fragmenting rupture and mixed tensile and shear failure modes, regardless of the material states tested. More testing is underway to determine the relationship between SSBD burst pressure and projectile velocity.

Introduction

Micro-meteoroid Orbital Debris (MMOD) is a growing problem in all earth orbits. After over fifty years of space launches by the government and the private sector there is a non-quantified and growing amount of debris orbiting the earth at over 7,800 km/s per second (17,500 mph) [1]. With human lives at risk, it is especially important to understand the effects of this debris on materials. In Las Cruces, New Mexico, at the National Aeronautics and Space Administration (NASA), White Sands Test Facility (WSTF) the Remote Hyper Velocity Test Laboratory (RHTL) has been testing the effects of Hypervelocity impacts with two stage light gas launchers since the early 1980's. These launchers compress Hydrogen gas to propel projectiles at near orbital velocities. The launcher is operated by loading a specific amount of launcher powder into the breach of the launcher. The launcher powder is ignited and the expanding gas from the powder drives a nylon piston down a pump tube filled with hydrogen, the hydrogen is compressed between the piston and a burst membrane or disk. Once the pressure is great enough, the disk bursts and a launch package consisting of a sabot and projectile is launched down a barrel. Once the launch package leaves the barrel and enters free flight the projectile and sabot are either centrifugally or aerodynamically separated. Then the sabot is stripped away with a Lexan® stripper plate. The projectile continues with minimal secondary debris and hits a target. The optimization of these launchers is a challenging endeavor since changes in each component have non-linear and interconnected variables that affect the performance of each surrounding component [2].

Background

Burst disks and petal valves are used in a variety of applications in aeroballistics. In the case of this experiment the SSBDs main function is typical, to couple the internal volumes of the launch tube to the pump tube and release high-pressure gas of a desired pressure from the pump tube to the barrel [1]. For the purposes of SSBDs the optimization of a burst pressure is in the hopes of increasing launcher efficiency, transmitting more energy to the launch package and therefore increasing eventual projectile velocity. At WSTF, on the 17-cal launchers, an aluminized Mylar® burst membrane is commonly used for day-to-day operations, not petal valves or bust disks.

Experimental

This project consisted of determining how to manufacture burst disks out of stainless steel shim stock, devising a fixture to reliably laser etch the surface of the SSBDs, determining parameters for the laser etching, test the SSBDs for reliability and calibrating them for burst pressure, implementing the SSBDs into the 17-cal launcher, modifying existing launcher components, and finally evaluating SSBD's effect on launcher performance.

Manufacturing

The disks are manufactured using annealed 316 series stainless steel shim stock thicknesses 0.178, 0.254, 0.305, and 0.381 mm (0.007, 0.010, 0.012, 0.015, and 0.020-in.) with sizes 0.178, 0.254 mm (0.007, 0.010-in.) manufactured with full hard 300 series stainless steel as well. Using wire EDM, the disks are machined in batches, by shearing uniform strips of stainless steel off larger sheets then stacking them on top of sacrificial aluminum plates. When the shim stock is sheared, the grain directionality resulting from plate rolling operations is carefully preserved, and the strips carefully stacked. Then the two sacrificial plates are clamped flat and tack welded together sandwiching the shim stock stack in-between. The tack welds prevent the aluminum plates and shim stock from bowing when end clamps are used to affix the shim stock sandwich in the EDM machine resulting in elliptical disks (Figure 1). EDM was chosen as the manufacturing method because it does not warp the disks during machining process, reproducibly manufactures relatively large numbers of nearly identical disks in the same batch and is highly accurate.

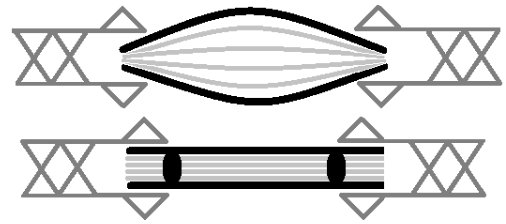

Figure 1. Compared side view diagrams of clamped/not tack welded plate sandwich (top) and clamped/tack welded plate sandwich (below). The dark gray structures on each side are end clamps, the thick black lines are the sacrificial aluminum plates, and the thin light gray lines are the shim stock strips. Note bowing of the shim on the top diagram vs. bottom diagram.

Figure 2. SSBD design showing the notch at the top disk in line with the grain direction of the shim stock.

The disk design has a notch in line with the grain rolling direction that integrates with the etching fixture to control grain rolling direction (Figure 2). As each disk is completed a slight burr is removed from the side of the disk with fine grit sand paper. The disk is sized to fit with a very tight tolerance to the inside of the Accelerated Region (AR) section and the size of the notch affects how well the disk seals hydrogen in the pump tube. The notch was designed to be the minimum resolution of the rapid prototype used to make the etching stand.

Etching Fixture

The etching fixture is designed using a 3-D modeling software package and is rapid prototyped from acrylonitrile butadiene styrene (ABS) plastic. The fixture has two versions; one with a protruding notch at 0º (Figure 3) and one with a protruding notch at 45º. The fixture accommodates an

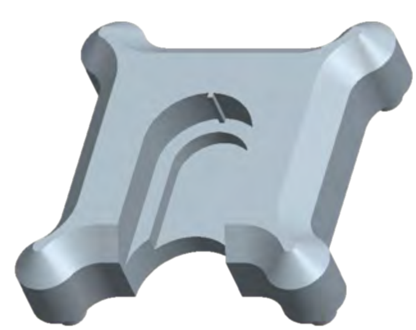

Figure 3. Final 0˚ etching stand.

aluminum heat sink to prevent the fixture from melting if the laser etching heats up a SSBD too much. It also makes a SSBD easier to remove while that SSBD is still hot after etching. The fixture also features two offset trenches, the bottom surface of the top trench supports the disk and the other trench makes the disk easier to remove. There are also four feet on the etching fixture that interlock with the regularly spaced accessory holes on the laser table providing minimum wobble of the fixture relative to the table, and allowing the laser to hit as close to the same place as possible on each disk.

Heat Sink

The heat sink is the result of the sacrificial aluminum plate. When the wire from the EDM process cuts through the sacrificial aluminum plates it makes thick aluminum disks at exactly the same dimensions as the SSBDs. The resulting aluminum disks are then machined in the middle to prevent contact between the back side of the affected etching area and the heat sink. The rationale for the heat sink design is to preventing the etching fixture from being melted by the disk while and after the disk is etched, and limit the contact of etching area underneath the disk with the heat sink.

Laser Etching

Laser etching was used to define the pedaling fracture pattern on blank disks. The parameters for etching have nearly infinite effective combinations. To preform more efficient testing it was decided to vary the number of laser runs for a fixed parameter instead of varying the number of laser parameters. The etcher had existing swaths of laser parameters on stainless steel coupon sheets. The fixed laser parameter used was selected from this swath coupon, and kept consistent for all of the tests. The distance between the top surface of the SSBD's and the laser table was recorded using a NASA calibrated digital Mitutoyo© caliper, and re-entered between each individual disk to ensure the focus the laser on the surface of each SSBD was as close to uniform between tests as possible.

Testing

The disks were burst in a pump system that applies hydrostatic pressure at a controlled rate of 1379 kPa per second (200 psi per second). The fixture consists of a sawed off barrel, AR shackle and AR coupler. The hydrostatic fixture diverges from the launcher with an adapter that connects the AR to the high pressure hydrostatic pump, instead of the hydrogen pump tube. The fixture is attached to the system using 0.64 cm (0.25") stainless steel coned and threaded nipple and high pressure stainless steel tubing from High Pressure Equipment Company©. Then the highest pressure seen by the pressure transducer, in the pump assembly, during the test was recorded as the burst pressure.

Implementation into the Launcher

In preliminary research shots after placing the SSBDs between AR section and the non-tapered barrel the SSBDs had holes punched in them sending the entire unsupported diameter of the disk touching the internal diameter of the barrel into the target. The AR section had to be modified to reduce the stress concentration between the barrel the disk. To accomplish the reduction of the stress concentrator, a special insert was designed with a radius facing the breach of the launcher blending down to the diameter of the barrel. The nomenclature used by WSTF for this insert is a "petal catcher" (Figure 4). The result was a consumable launcher component that allows the petals to bend over the radius of the petal catcher without dramatically blocking the flow of high pressure hydrogen, and without breaking, or damaging the barrel. When the petal catcher becomes too damaged to use it is simply replaced, without honing or any additional machining to the barrel. The AR had to be modified to accommodate the added thickness of the SSBD and the petal catcher while still allowing the barrel to seal properly against the down range side of the AR (Figure 5). Also the radius on a given petal catcher can be designed to change the unsupported area behind the etched SSBD. This effect is described later.

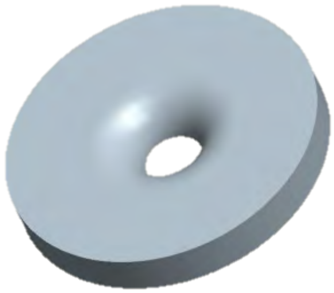

Figure 4. Breach side of petal catcher showing radius geometry.

Figure 5. Petal catcher (middle) inserted toward the breach into the modified AR section showing the center of the etched SSBD underneath.

Experimental Design Planning

The test matrix was planned using design of experiments (DOE) methods so that the data would efficiently estimate the coefficients of an equation that could be used to predict the median value of future test runs. In addition, it was planned so that variability could also be examined to determine conditions over which the petal valve burst pressure would be least variable.

An equation that adequately predicted burst pressure based solely on material thickness and depth of score was determined using linear regression analysis. As expected, increasing metal thickness and decreasing depth of score resulted in predictably increased burst pressure. It was shown that use of a heat sink and orientation of the score compared to the grain of the metal had little or no effect on burst pressure but may have an effect on variability. Full-hard metal appears to result in more highly-variable burst pressures. The effect of differences between lots of metal was not explored.

Planning

The goal of this experiment was to determine a combination of various factors that resulted in a consistent rupture pressure with low probability of breaking off pieces of the petals on the disk during and after rupture. The testable statement of problem, then, was:

1. To find an equation that related the various input factors to the desired responses, and
2. To find settings of factors that maximized robustness, and minimized variability.

In other words, it was not enough just to describe the relationship between the factors and responses. It was also desirable to achieve good consistency between firings of the launcher, a key attribute of excellent test equipment.

The test was planned using design of experiments (DOE) principles [3]. DOE is a set of methods and tools that provide an efficient, systems-engineering based framework for designing experiments that achieve a goal with the most efficient use of the experimental data. Here, it meant that a sizeable design space – range of input factor settings – be explored. The requirement for determining robustness mandated a somewhat larger number of runs than might ordinarily be desirable to characterize variability; in essence, replicates were important. It was also believed that the unexplainable variability was considerable. Because statistical significance essentially requires being able to find a signal (effect of a factor on a response) over noise (unexplained, or residual, variability), this necessitated a certain number of test runs (samples) to amplify the signal over the expected noise level. The number of samples required was estimated using DOE tools. The methods also allow an experimenter to define an experiment so that it will determine interactions (synergies) between factors, a condition expected to occur here.

The following responses were important:

- Burst pressure; measured in psi by a pressure gage that measured at 1 Hz
  - The slow response rate was expected to increase variability
  - Goals: minimize variability; find predictors to hit a specific value
- Pieces – count; will have to apply a guess or have to catch pieces somehow
  - Goal: consistent zero

- Fracture shape; some kind of photo record and reasonably precise rating
    - Goal: petal-looking appearance

The following factors were believed to be important in affecting the responses:

- Laser runs (proxy for depth of score)
- Material thickness
    - Thickness and laser runs were correlated (see further text)
- Material Type (full hard v annealed)
- Alignment of score in barrel (centered v offset)
- Grain direction compared to score direction (orthogonal v diagonal)
- Heat sink (with v without)

There were a number of potential factors regarding the laser used to produce the petal valve score that were held constant. These included laser speed, pulse frequency, lamp current, height, focus, wobble frequency and the index line width.

Metal thickness was correlated with number of laser runs. That is, thinner material could not be scored as deeply as thicker, and thicker material was expected not to be as sensitive to a shallow score depth as thinner material. A set of test runs were performed to determine the approximate number of laser runs that would burn through a given SSBD metal thickness. It was found that the square root of number of laser runs to burn through correlated reasonably well with SSBD metal thickness. An effective range of laser runs for each thickness was determined. The number of laser runs was turned into a percent of laser runs required to achieve SSBD burn through.

This allowed a test matrix that was reasonably orthogonal on material thickness and a proxy measure for depth of score to be constructed. Orthogonality here refers to the correlation between the two factors. If correlation is high, it is more difficult to ascertain the contribution to pressure due to each of the factors – noise is increased, efficiency is decreased. When the factors are not correlated – orthogonal – the effect of each can be estimated completely in isolation from the other factors.

One factor, barrel taper (tapered v not tapered), referred the having a petal catcher or not during testing. The petal catcher required to make the tapered barrel configuration had un-quantified effects on burst pressure that were interesting to the experiment. A number of runs without using a petal catcher were planned and designated as the not-tapered barrel configuration. The experiment was planned so that all of the data, both the tapered and not-tapered data, could be used to reduce uncertainty during the analyses.

A test matrix, i.e. plan showing the list of the intended test runs, the factor settings for each run and the order in which each run would be performed, was set before any testing was performed. This original matrix was designed using Design Expert® software version 8. A set of data from a small exploratory test was used to estimate range of size of effects and variability. The matrix was designed to give a high probability (>80% power) [4] of identifying quadratic effects of thickness, number of laser runs and up to second-order interactions between a few factors (Figure 6)(Table 1). The software optimized the test matrix using the D-optimality criterion, which chooses the test matrix of independent variables X based on maximizing the determinant of the X'X matrix [5]. The resulting data could be expected to allow a minimally uncertain estimate of the parameters for the resulting linear regression model, desirable for prediction using the model.

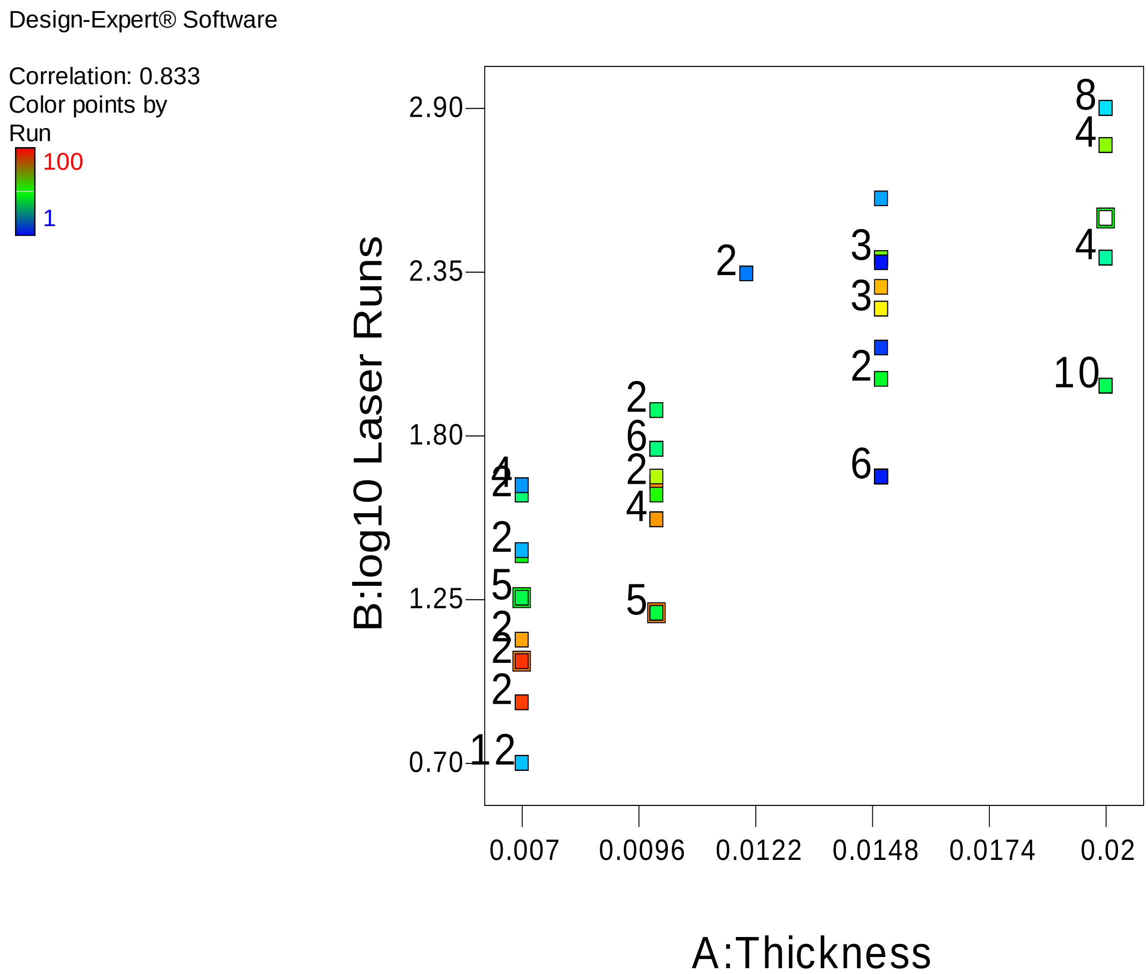

Figure 6. Arrangement of Test Trials by number of laser runs and material thickness. Integers indicate number of test articles at that combination of factors.

The test matrices were completely randomized (save for the variable petal catcher variable, which was changed once). This ensured that any systematic trend due to a non-experimental variable – degradation of the test fixture, for instance – or other nuisance variable would not systematically correlate with any test factor. This provided increased protection that any outside influence on the data would end up in the unexplained noise instead of masquerading as some factor.

A small number of in-situ changes were made to the test matrix during testing. The variability of number of laser runs to achieve burn through was greater than estimated during this pretest, resulting in a lower upper limit on laser runs. This issue was uncovered partway through testing. Also a misunderstanding on available material constrained the number of tests at particular thicknesses. Each change was made by taking the as-performed test matrix and results from testing to that point and using an algorithm in the Design Expert® software to construct an augmentation to the existing tests again using the D-optimality criterion. While it isn't ideal to make substantial changes midway through, using this method to adapt the test matrix resulted in preserving considerable efficiency in achieving test goals.

Table 1. Burst matrix. Thickness is expressed in units of inches and burst pressure is expressed in units of psi. 'NT' represents the 'Barrel Not Tapered' configuration, and 'BT' represents the 'Barrel Tapered' configuration. Failure mode describes whether or not the disk failed due to the etch: "Etch", burned through during etching: "Burn", or the unsupported area of the disk was punched out at rupture: "Punch".

Run Order	Block	Thickness	Laser Runs	Grain Direction	Heat Sink	Hardness	Burst Pressure	Failure Mode
1	NT	0.007	43	45	Without	Annealed	3236.4	Etch
2	NT	0.02	251	0	With	Annealed	23800	Etch
3	NT	0.015	242	0	With	Annealed	8018.2	Etch
4	NT	0.015	46	0	With	Annealed	21545.5	Etch
5	NT	0.02	800	45	Without	Annealed	10109.1	Burn
6	NT	0.02	93	45	With	Annealed	27436.4	Etch
7	NT	0.015	125	0	With	Annealed	12218.2	Etch
8	NT	0.007	5	45	With	Annealed	13472.7	Punch
9	NT	0.007	26	0	Without	Annealed	6181.8	Etch
10	NT	0.015	46	0	With	Annealed	20054.5	Etch
11	NT	0.02	800	45	With	Annealed	10054.5	Burn
12	NT	0.012	222	45	With	Annealed	2909.1	Etch
13	NT	0.012	222	45	With	Annealed	2981.8	Etch
14	NT	0.007	5	45	With	Annealed	13490.9	Punch
15	NT	0.015	46	45	Without	Annealed	19981.8	Etch
16	NT	0.007	43	0	With	Annealed	3436.4	Etch
17	NT	0.015	397	45	Without	Annealed	4400	Burn
18	NT	0.007	5	0	Without	Annealed	13600	Punch
19	NT	0.007	26	0	Without	Annealed	5327.3	Etch
20	NT	0.007	5	45	Without	Annealed	13363.6	Punch
21	NT	0.02	251	45	With	Annealed	19327.3	Etch
22	NT	0.02	251	0	With	Annealed	19345.5	Etch
23	NT	0.02	800	0	Without	Annealed	8563.6	Burn
24	NT	0.02	800	45	Without	Annealed	9654.5	Burn
25	NT	0.007	43	45	Without	Annealed	3000	Etch
26	NT	0.007	43	0	With	Annealed	5272.7	Etch

27	NT	0.02	800	0	With	Full Hard	N/A	N/A
28	NT	0.02	800	0	Without	Annealed	9781.8	Burn
29	NT	0.007	5	0	Without	Annealed	13309.1	Punch
30	NT	0.02	93	45	Without	Annealed	26527.3	Etch
31	NT	0.015	46	45	Without	Full Hard	N/A	N/A
32	NT	0.02	93	45	Without	Annealed	26090.9	Etch
33	NT	0.007	5	45	Without	Annealed	13363.4	Punch
34	NT	0.02	93	45	Without	Annealed	26163.6	Etch
35	NT	0.02	800	0	Without	Annealed	9563.6	Burn
36	NT	0.02	800	0	With	Full Hard	N/A	N/A
37	NT	0.02	800	45	With	Annealed	10072.7	Burn
38	NT	0.02	251	0	Without	Annealed	18036.4	Etch
39	NT	0.02	800	45	With	Annealed	8836.4	Burn
40	BT	0.01	57	45	Without	Full Hard	1401	Etch
41	BT	0.02	93	0	Without	Annealed	13090.9	Etch
42	BT	0.01	57	45	With	Full Hard	1927.3	Etch
43	BT	0.007	40	0	Without	Annealed	1290.9	Etch
44	BT	0.01	77	45	Without	Annealed	1127.3	Etch
45	BT	0.02	93	0	Without	Annealed	12545.5	Etch
46	BT	0.02	93	0	With	Annealed	12872.7	Etch
47	BT	0.007	18	45	With	Annealed	8036.4	Etch
48	BT	0.01	16	0	Without	Annealed	14381.8	Etch
49	BT	0.007	18	0	Without	Full Hard	5290.9	Etch
50	BT	0.015	98	0	Without	Annealed	7200	Etch
51	BT	0.015	250	0	Without	Annealed	2618.2	Etch
52	BT	0.007	25	0	Without	Annealed	963.6	Etch
53	BT	0.007	18	0	With	Full Hard	1236.4	Etch
54	BT	0.015	46	45	Without	Annealed	10618.2	Etch
55	BT	0.02	341	45	Without	Annealed	1927.3	Etch
56	BT	0.02	93	45	With	Annealed	13072.7	Etch
57	BT	0.01	40	0	Without	Annealed	3545.5	Etch
59	BT	0.02	93	0	With	Annealed	12145.5	Etch
60	BT	0.015	169	45	Without	Annealed	3109.1	Etch
61	BT	0.01	77	0	With	Annealed	1090.9	Etch
62	BT	0.007	5	0	Without	Full Hard	11363.6	Etch
63	BT	0.015	250	0	With	Annealed	2945.5	Etch
64	BT	0.02	600	0	With	Annealed	3381.8	Etch
65	BT	0.007	5	45	With	Full Hard	11654.5	Etch
67	BT	0.015	250	45	Without	Annealed	2127.3	Burn
69	BT	0.007	18	45	With	Annealed	6727.3	Etch
70	BT	0.01	16	45	Without	Full Hard	15054.5	Etch
71	BT	0.02	600	0	With	Annealed	2945.5	Etch

72	BT	0.015	169	45	Without	Annealed	3872.7	Etch
73	BT	0.007	40	45	With	Annealed	2909.1	Etch
74	BT	0.007	5	0	With	Annealed	11200	Etch
75	BT	0.01	77	45	Without	Annealed	4290.9	Etch
76	BT	0.01	16	45	With	Annealed	11363.3	Etch
77	BT	0.015	46	0	Without	Annealed	11054.5	Etch
78	BT	0.007	5	0	With	Annealed	8727.3	Etch
79	BT	0.015	46	45	With	Annealed	10927.3	Etch
80	BT	0.007	5	45	Without	Annealed	11327	Etch
81	BT	0.01	57	0	With	Full Hard	2418.2	Etch
82	BT	0.02	93	45	With	Annealed	11389.1	Etch
83	BT	0.015	169	45	Without	Annealed	4145.5	Etch
84	BT	0.015	98	45	With	Annealed	5981.8	Etch
85	BT	0.02	600	45	Without	Annealed	3109.1	Etch
86	BT	0.02	600	0	With	Annealed	2890.9	Etch
87	BT	0.01	16	0	With	Full Hard	10872.7	Etch
89	BT	0.007	18	45	Without	Full Hard	2545.5	Etch
90	BT	0.015	200	0	Without	Annealed	2600	Etch
91	BT	0.01	57	0	With	Annealed	2418.2	Etch
92	BT	0.007	13	0	Without	Annealed	3890.9	Etch
93	BT	0.01	33	45	Without	Annealed	5836.4	Etch
94	BT	0.01	44	45	With	Annealed	4690.9	Etch
95	BT	0.01	16	0	With	Full Hard	4727.3	Etch
96	BT	0.007	11	0	Without	Full Hard	1090.9	Etch
97	BT	0.007	13	0	Without	Annealed	6781.8	Etch
98	BT	0.01	57	0	Without	Full Hard	1472.7	Etch
99	BT	0.01	57	45	Without	Annealed	3418.2	Etch
100	BT	0.01	44	0	Without	Annealed	4236.4	Etch
101	BT	0.007	8	0	With	Full Hard	9545.5	Etch
102	BT	0.007	8	45	Without	Full Hard	6945.5	Etch
103	BT	0.007	11	45	With	Annealed	9200	Etch
104	BT	0.01	33	0	With	Annealed	6618.2	Etch
105	BT	0.007	5	45	Without	Annealed	11400	Etch
106	BT	0.01	33	45	Without	Full Hard	5563.6	Etch
107	BT	0.01	33	45	With	Annealed	6981.8	Etch

Analysis and Results

The resulting data were analyzed using several statistics packages, including Design Expert®, JMP® version 9 and Statgraphics Centurion® version 16. The general analysis method was ANOVA combined with a multiple regression, as described in Montgomery [3]. Three packages were used due to the complexity of the data and enhanced features in each suite particularly in graphical analysis. Quantitative analyses due to each suite resulted in the same conclusions. Statistical significance was set at 0.05.

It was found that the logarithm of the number of laser runs worked better as a linear predictor of burst pressure than the untransformed number of laser runs. A pattern in the residuals (observed value minus model-predicted value) suggesting a missing term or effect was greatly lessened.

It was found that barrel configuration made a difference. The regression model shown here will thus give two response surfaces, one for each level of this variable (Figure 7, 8).

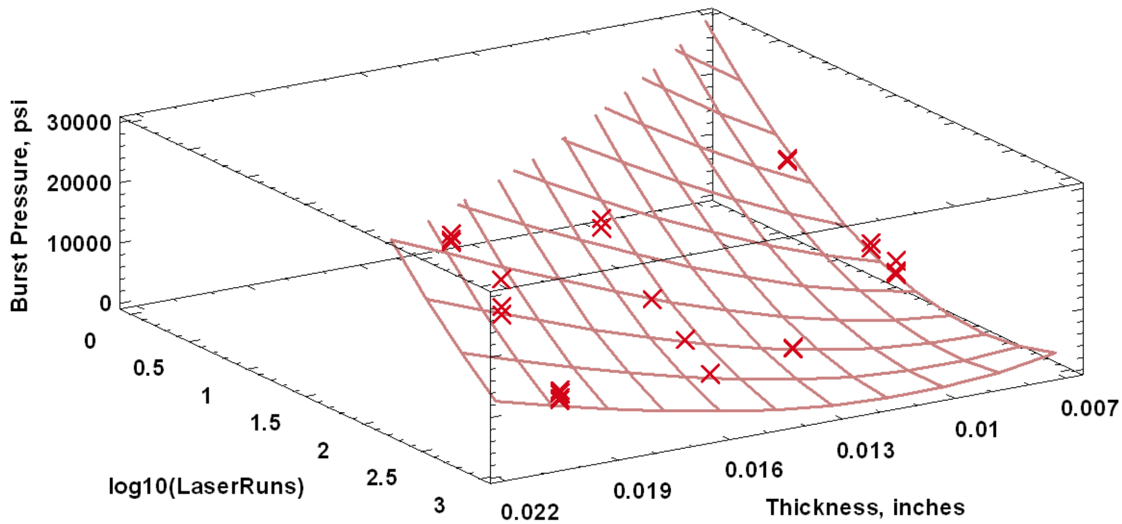

Figure 7. Estimated response surface (regression model) for the Barrel Not Tapered (red) data.

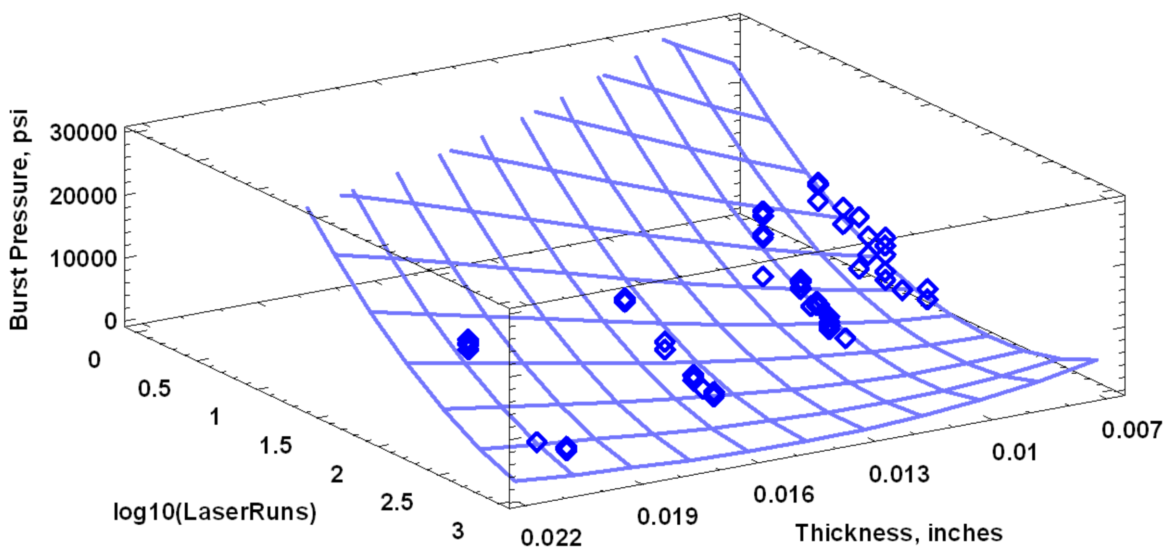

Figure 8. Response surface (regression model) for the Barrel Tapered (blue) data.

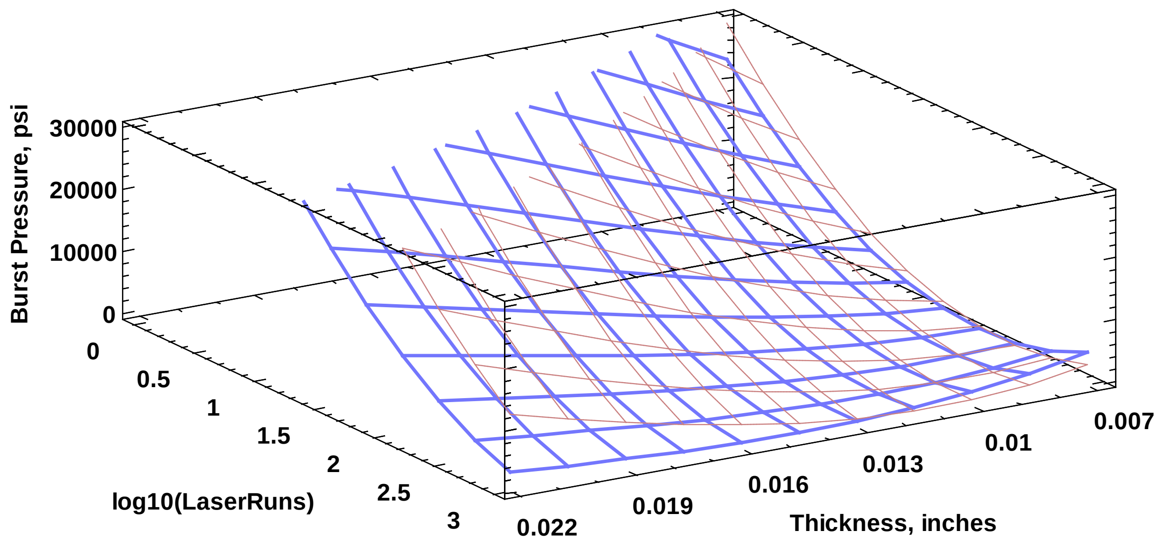

Figure 9. Overlain response surfaces. Barrel Tapered (blue), Barrel Not Tapered (red). Note the difference between the model predictions.

There is a clear relationship between thickness, laser runs and burst pressure. These graphs (Figure 7, 8, 9) also show that the non-tapered barrel results in a higher burst pressure for a given thickness. It is important to note that each response surface is directly dependent on the geometry of the petal catcher. Also notice that the slope of the change in burst pressure seen between the two surfaces is not linear. This non-linearity describes the effect of petal catcher geometry due to the difference in unsupported SSBD area with changing radius. It might be that if a high burst pressure is desirable, then, it is beneficial to look at smaller petal catcher radius design. However, from this point, much of the focus will be on the Tapered Barrel data since this is the condition initially tried in the launcher successfully.

The response surfaces or both Tapered and Non-Tapered data (Figure 7, 8) describe non-credible behavior in some areas of the graphs; witness the 0.007" thickness at 3 $\log_{10}$ laser runs, where the prediction is that the burst pressure is expected to begin to increase. Note that there is no data in this region. The regression model (Figure 10) is assumed to approximate the actual physical function driving burst pressure, but not exactly match it. The fit within the range of the data is fairly good. It is never assumed that the expression will match the true physics of the situation very far beyond the range of the data without a reason for doing so. The prediction in this region is thus not only not credible, but also not important.

```
⎛103.249502102847                                                                              ⎞2
⎜                          ⎛"Barrel Not Tapered"     ⇒ 17.1042241737301  ⎞
⎜+ Match  ⎛Block ⎞         ⎜"Barrel Tapered"         ⇒ -17.10422417373   ⎟
⎜                          ⎝else                     ⇒ 0                 ⎠
⎜+ 9543.26945319146      * A:Thickness
⎜+ ⎛A:Thickness   -0.01268 ⎞
⎜ *⎛⎛A:Thickness   -0.01268 ⎞* -176358.10321179      ⎞
⎜+ -32.064362761126      * Log ⎛B:LaserRuns ⎞
⎜                          ⎛"Barrel Not Tapered"     ⇒ ⎛A:Thickness   -0.01268 ⎞* 1431.96684617486 ⎞
⎜+ Match  ⎛Block ⎞         ⎜"Barrel Tapered"         ⇒ ⎛A:Thickness   -0.01268 ⎞* -1431.9668461749 ⎟
⎝                          ⎝else                     ⇒ 0                                         ⎠⎠
```

Figure 10. Shows a graphic version of the full regression prediction expression discussed above with logic.

Reduced to the form that predicts the expected response for the tapered-barrel design is Equation 1:

$$32.064*\log \qquad]2 \qquad (1)$$

Equation 1 was used to compare actual burst pressure to predicted burst pressure for each tapered barrel data point (Figure 11). The resulting data was linearly fit with a R^2 value of 0.9 demonstrating the capability of the equation to predict burst pressure using only SSBD thickness and number of laser runs.

The analysis of variance (ANOVA) results (Table 2) find the significance of the model to be quite high. All of the coefficients were determined significant at >0.0001 except for Thickness squared, which was significant at >0.02.

Table 2. Analysis of Variance Results

Source	DF	Sum of Squares	Mean Square	F Ratio
Model	5	102092.58	20418.5	163.7592
Error	94	11720.51	124.7	**Prob > F**
C. Total	99	113813.09		<.0001*

The R^2 value below (Table 3) matches the adjusted R^2 value below it quite well, indicating a reasonably well-specified model (essentially, there aren't too many parameters in the model). The lack-of-fit statistic is 0.1524 (Table 4), a value that suggests that the model fits the data well enough. Values below 0.05 indicate a model that doesn't fit the data adequately.

Table 3. Summary of Fit

Source	Value
RSquare	**0.89702**
RSquare Adj	0.891542
Observations	100

Table 4. Lack of Fit. DF is the degrees of freedom.

Source	DF	Sum of Squares	Mean Square	F Ratio
Lack Of Fit	27	4159.841	154.068	1.3653
Pure Error	67	7560.665	112.846	**Prob > F**
Total Error	94	11720.506		**0.1524**

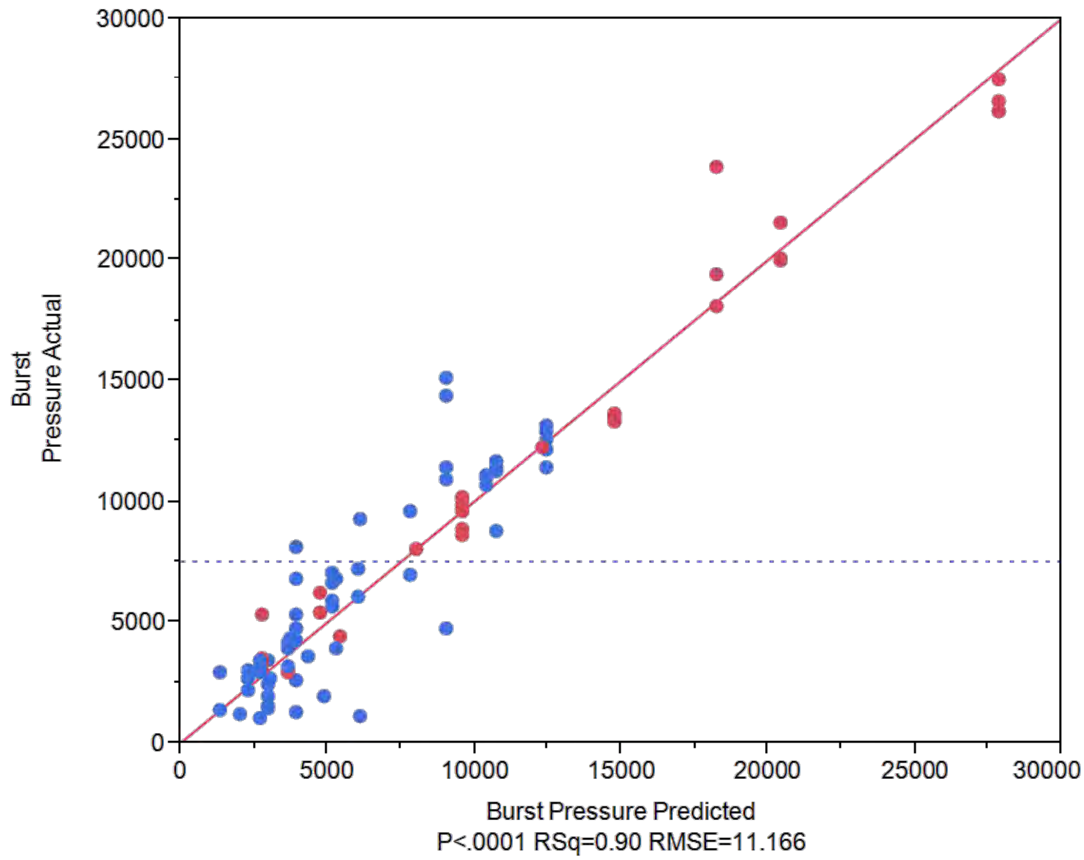

Figure 11. Compares actual burst pressure to predicted burst pressure for each tapered barrel data point using Equation 1. Red data is full hard SSBDs, blue data is annealed SSBDs, all pressure is expressed in psi.

The effects of the remaining factors were found to be not significant above the noise (not significant at the 0.05 significance level). In addition, several factors affected run-to-run repeatability in burst pressure. Following is a review of these factors.

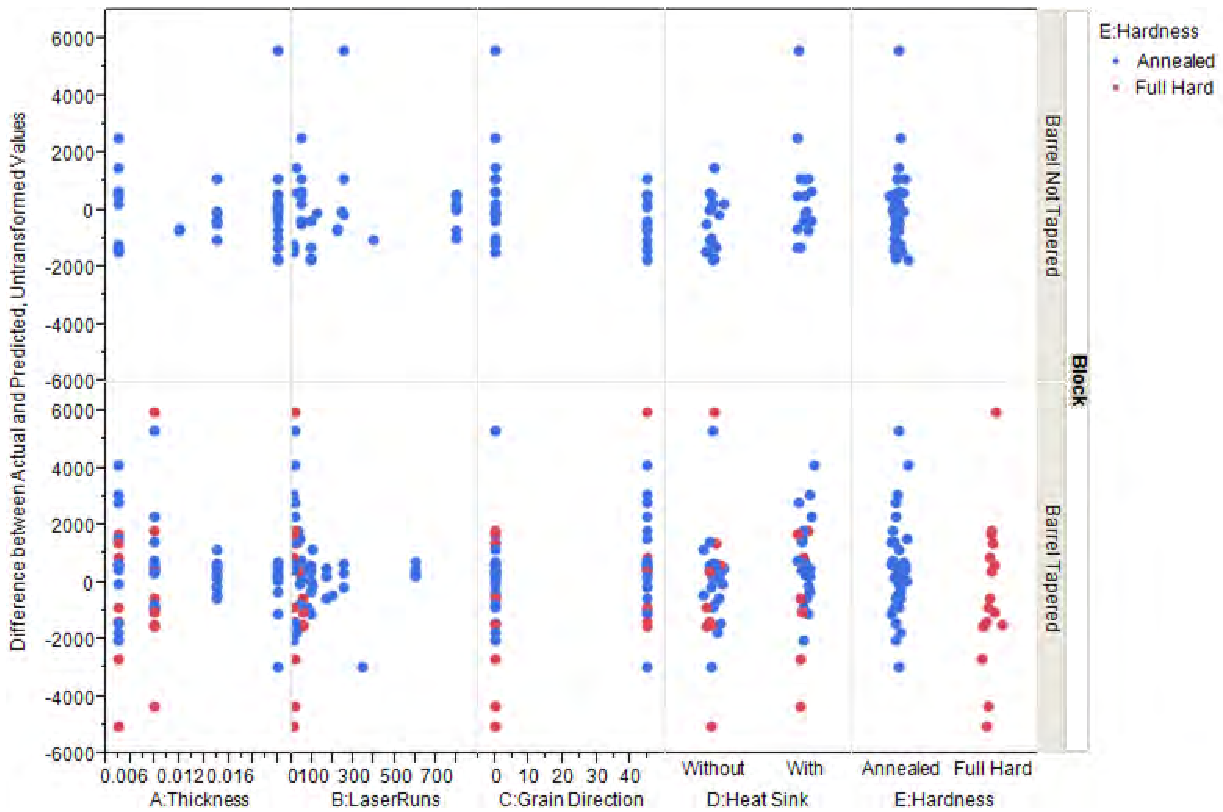

Figure 12. Multiple plots showing various parsing of the data, comparing the untransformed actual and predicted values of burst pressure (psi) with experiment response variables.

Figure 12 plots the residuals of the regression equation. Again, residuals are the actual observation values for each point minus the model's prediction for that observation. They represent the spread of the data around the model prediction. The mean of all the residuals is zero. The units on the left axis are psi. Negative values represent observations below the model prediction; positive values are observations above the model response surface plane. The residuals are divided here into non-tapered (top tier of graphs) and tapered (bottom tier) barrel runs. Each cell contains the complete set of either tapered or non-tapered barrel residuals graphed by whatever is on the x-axis. The full-hard material is colored differently, in red. For instance, the bottom left cell represents the tapered-barrel run residuals plotted by the material thickness in inches. The data is roughly centered at zero, though it might be argued that there is a positive bias to the residuals. In fact, the complete Barrel Tapered dataset is centered at very nearly zero, but there are proven and potential features in the data that affect this visual analysis.

One of those is a cone-shaped pattern in the data's spread. Thin material shows more variability than thick material. This is germane to the problem at hand – clearly, thinner material results in greater variability, so if an experimenter wants the launcher to fire at a repeatable value, a thicker burst disk might be appropriate. It also appears clear that there are some very highly variable individual observations, some which may demonstrably represent outliers. These extreme values seem to be full-hard material. While there did not appear to be a significant effect of full-hard v annealed metal in predicting mean pressure at burst, it does appear that full-hard material may result in less-predictable burst values around that mean. Use of annealed material is recommended.

The variability by material thickness does not appear to occur in the Barrel Not Tapered data. Note that because randomization was restricted and all of these runs were performed first, while some bugs may have been being worked through, this may not be a true finding. However, this statement may be true: the process could be more robust to thickness changes with a non-tapered barrel than with tapered. If this is a radius dependent finding that could potentially translate to real tests on the launcher, this might bear additional study. Likewise, the graph of tapered-barrel residuals v number of laser runs shows a much more pronounced taper in the spread. It appears possible that the apparent outliers attributed to full-hard material may actually be due to the small number of laser runs (as few as 5). The recommendation here would be to stay away from conditions where fewer insufficient laser runs will be applied to cause SSBD failure along the etch. However, again, it is possible that the non-tapered barrel data shows a more-robust response to number of laser runs or that this is an artifact of the smaller number of samples.

The grain direction plots for the tapered data show a possible difference between the orthogonal (0˚) and diagonal (45˚) orientation of the scores. It might be an interesting difference in engineering terms, perhaps on the magnitude of 1000 psi. However, the signal of the effect of grain direction was large in comparison to the noise in the data, so grain direction did not show up as a significant factor in the analysis. The small amount of data collected for full-hard material suggests that grain direction might make more difference for that material, but the dataset is too small to be sure. If someone's goal is to maximize burst pressure, maintaining a 45˚ grain direction might not hurt. However, while the variability in the two subsets of the data were not statistically significantly different, it is possible that the variability in the 0˚ data was less than for the 45˚. Overall, because variability minimization is important, it is recommended that controlling the scoring of the material orthogonal to the grain direction might be beneficial.

The effect of heat sink appears not to be particularly important. One might make the same arguments as for grain direction. Statically it is recommended that no heat sink be used; it appears this will either have no effect or reduce variability. However physically, since the etching stand can melt without a heat sink, it has benefits when used.

Not shown in this graph is number of fragments produced. There were only a handful of petal valves that produced fragments. All of these trials were associated with 0.007" thick material with 5 laser runs. Again, the recommendation is to avoid thin metal with a shallow score depth.

The effect of metal lot was completely confounded with thickness. Some systematic variability associated with thickness was seen in the data. Some lot-to-lot variability can be expected, and can be expected to have biased the coefficient estimates. The magnitude is unknown.

Fracture mechanics

Fracture surface images were taken with a scanning electron microscope at NASA WSTF by the scientists in the Materials Technology Group. Fractographic evidence of ductile overload, via a mixture between tensile and shear modes, was adjacent to the laser affected zone in both full hardened and annealed stress states (Figure 13, 14, 15). These ductile failure modes, exhibiting classic evidence of plasticity through the transgranular microvoid coalescence mechanism [6,7], are the expected fracture mode of an austenitic SS alloy, and are the complete opposite end of the spectrum from a brittle fracture mode. A brittle fracture mode in this application would be catastrophic to the quality of the shot because of the fragmentation potential of a brittle material response. Throughout out hydrostatic burst testing, in this study, and to date dynamic testing in the launcher no brittle material responses have been witnessed in SSBDs. However, on cannot rule out the potential for such failures to occur in the future.

Laser etching was very effective at notching the surface of the SSBD. Nearly all of the etched SSBDs demonstrated induced fracture along the etch with the number of laser runs prescribed in the DOE. The disks that did not fracture along the etch at failure did not have sufficient number of laser runs to cause a user defined fracture initiation path. With regards to grain direction, Figure 15 demonstrates the effectiveness of the SSBD manufacturing method at preserving grain direction from machine shop, etching stand, laser table to laser etch. Even though laser etching was very effective at scoring the SSBDs there were a couple of manufacturing anomalies that are worth noting. Figure 17 as opposed to Figure 16 shows a periodic stress concentrator that forms on the surface of the laser etch. Since the aim of the burst disk is to cause fracture along a designated path, these holes may not be detrimental. Also the holes do not penetrate the SSBD thickness, so they appear to have mostly beneficial effects.

Overall, the laser etching process is very effective at causing fracture along a designated fracture path, with minimum debris. This method has proven to work in initial firings in the launcher and further research is currently underway.

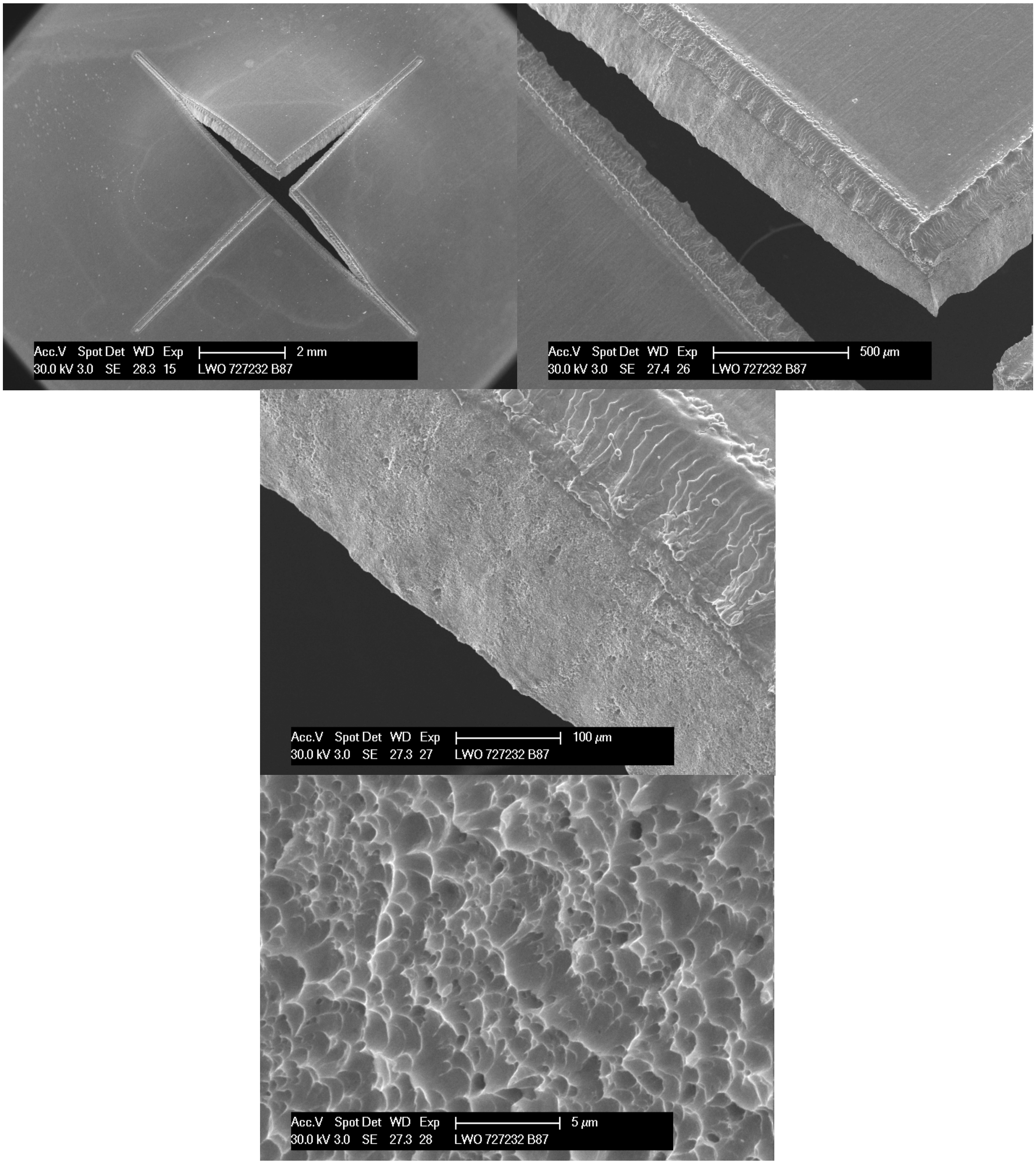

Figure 13. Hydrostatically burst disk showing enhanced detail moving right to left of fracture surface along the etch. On the bottom right notice the dimpled fracture surface, indicating ductile overload via transgranular microvoid coalesence.

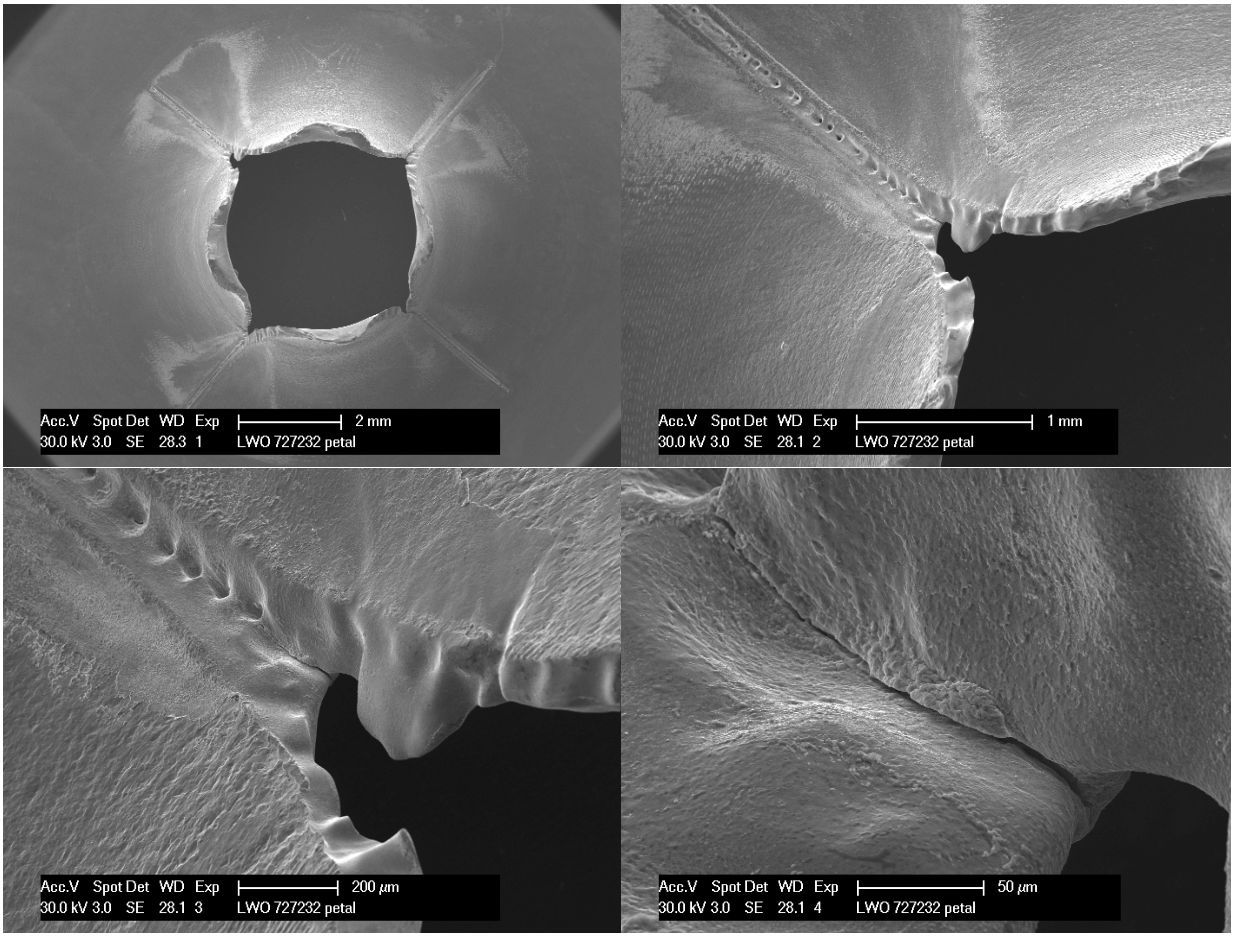

Figure 14. Disk dynamically burst, in the launcher, showing enhanced detail moving left to right of the upper right fracture surface. Note eroded fracture surfaces but overall ductile response of the material.

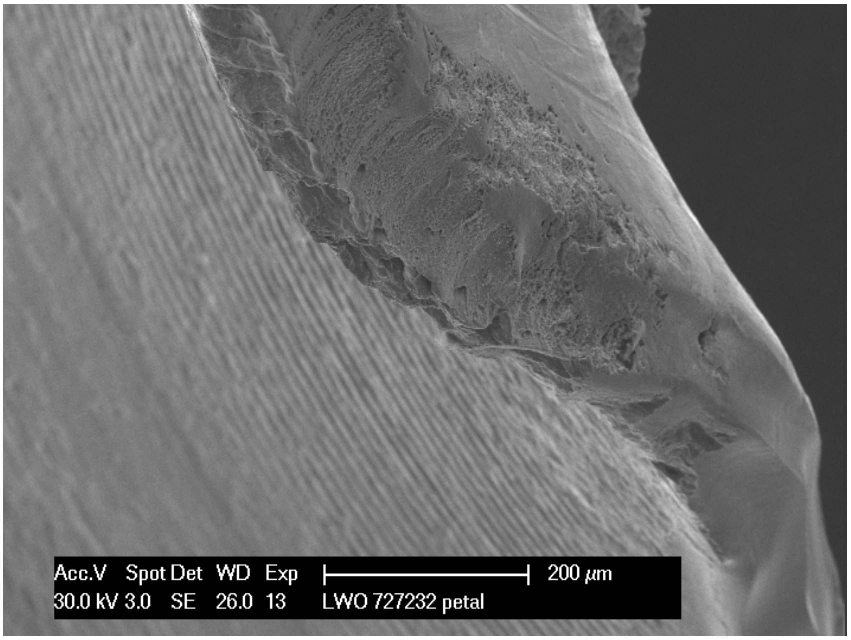

Figure 15. Fractographic shows the eroded surface on the bottom edge of the right most petal on the dynamically burst SSBD. Overall view shown in Figure 13 (top right).

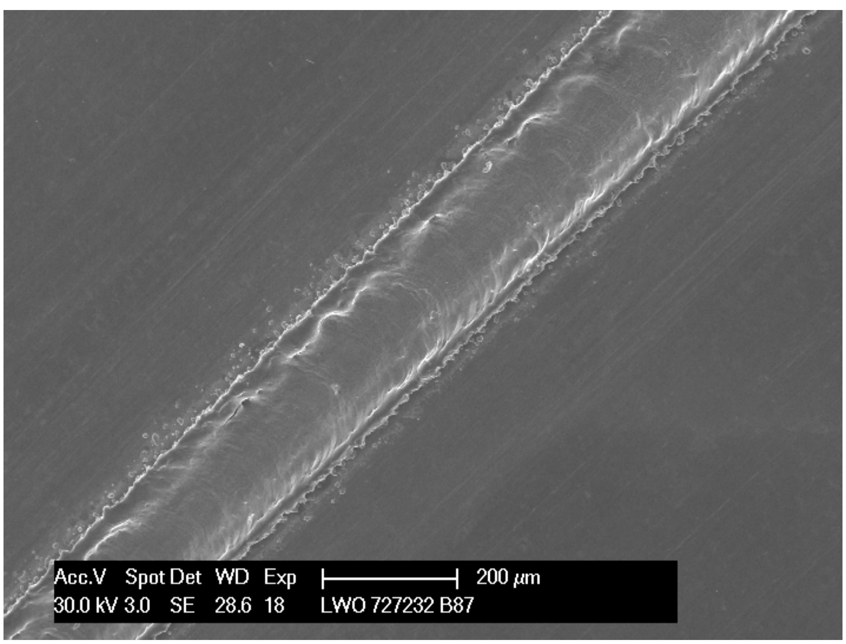

Figure 16. Shows a smooth laser etch parallel to the grain rolling direction.

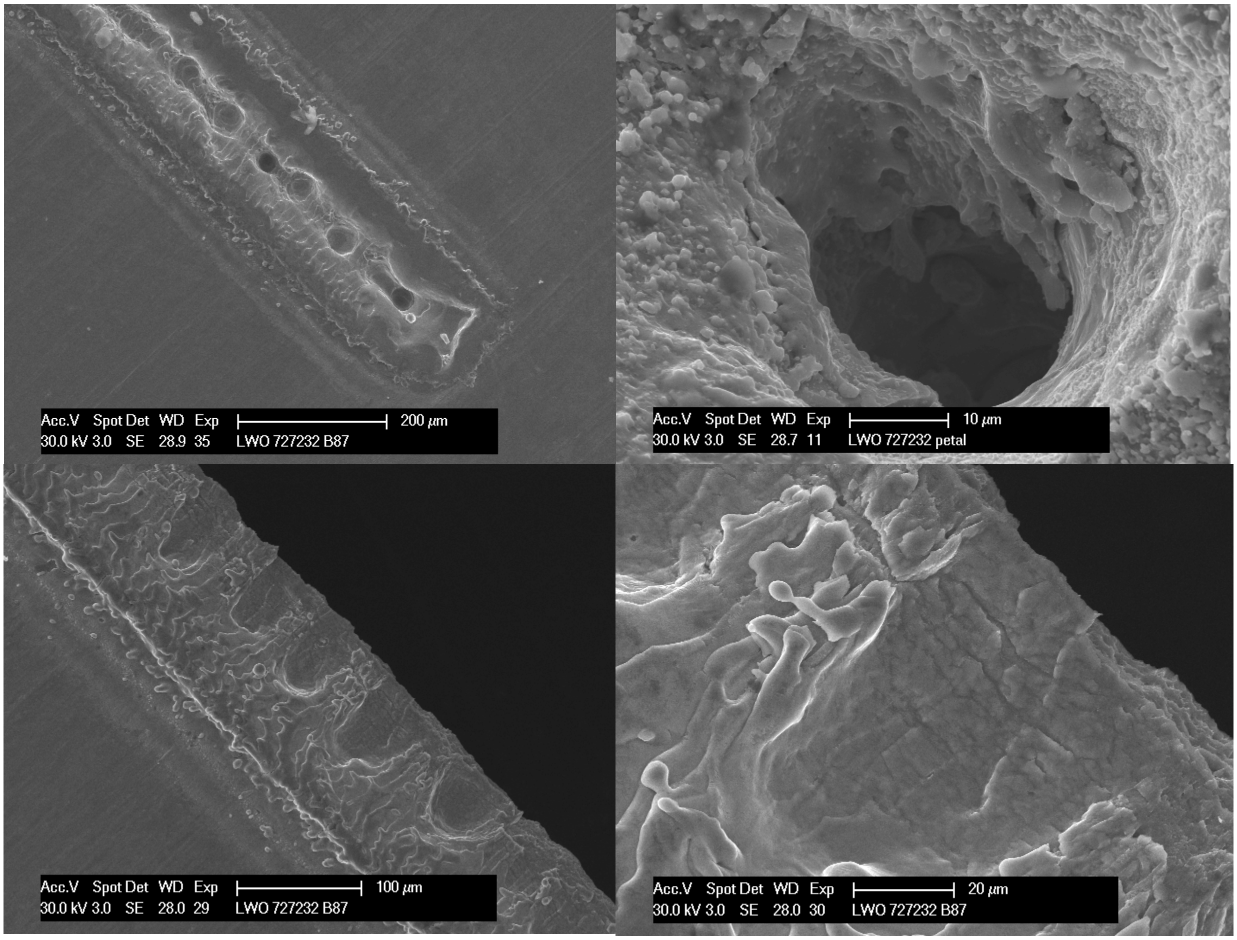

Figure 17. Shows a periodic etching anomaly that appears, sometimes but not always, on etches perpendicular to the grain direction. Top left to right top shows non-fractured etch and enlarged periodic hole. Bottom left to right shows anomalies on a post fractured etch then enlarged. Note the etch images shown on top are from different regions of the same SSBD shown on bottom.

Future Work

In the future, there is much more testing that could be done on SSBDs. First, different laser parameters may allow less runs and decrease manufacturing complexity and errors. Second, different materials choices may respond to the laser etching and be more practical for implementation into the launcher. Third, additional dynamic testing in the launcher needs to be modeled, accomplished and evaluated [8]. Fourth, performance metrics such as SSBD opening time would be very useful in design. An example of such research is quantifying the pressure shock wave between the moving piston and burst disk surface preformed at the University of British Columbia [9]. Fifth, a comparison of manufacturing methods looking into alternative disk manufacturing (e.g. punching) and petal manufacturing (e.g. diamond scoring, plunge EDM, precision milling, etc.) could be performed. Sixth, there is the potential for scaling up SSBD manufacturing methods for larger launchers, since laser etching works for thin samples. However laser machining might be less practical on larger samples since more powerful lasers are required. Finally, conducting more experiments to model and determine the effect of petal catcher radius on burst pressure and SSBD fracture response would be useful for future petal catcher designs [10]. Also knowing the effects of petal catcher radius factors would help enable the scaling of this research up or down in other launcher applications.

Conclusion

Laser etched Stainless Steel Burst Disks (SSBD) ranging between 0.178 mm (0.007-in.) and 0.508mm (0.020-in.) thick were designed for use in a 17-caliber two-stage light gas launcher. Wire electrical discharge machining (EDM) and laser etching were used to manufacture these SSBDs. A replaceable insert was designed to go between the SSDB and the barrel. This insert reduced the stress concentration between the SSBD and the barrel, providing a place for the petals of the SSDB to open, and protecting the rifling on the inside of the barrel. A design of experiments was implemented to test and characterize the burst characteristics of SSBDs. Extensive hydrostatic burst testing of the SSBDs was performed to complete the design of experiments study of one-hundred and seven hydrostatic burst tests. The experiment resulted in the quantification of the relationship between SSBD thickness, laser etch parameters, and desired burst pressure. Of the factors investigated only thickness and number of laser runs were needed to develop a mathematical relationship predicting hydrostatic burst pressure of disks using the same barrel configuration with an R^2 value of 0.89. The fracture surfaces of two representative SSBD bursts were then investigated with a scanning electron microscope; one burst hydrostatically in a fixture and another dynamically in the launcher. The fracture analysis verified that both burst conditions resulted in a ductile overload failure indicated by transgranular microvoid coalescence. Non-fragmenting rupture and mixed tensile and shear failure modes, were observed regardless of the material states tested. After firing initial shots in the launcher and using these new SSBDs, higher than expected velocities for a given powder load and launch package mass were recorded. More research is being conducted to determine the effect of these SSBDs on overall launcher efficiency.

Acknowledgement—The authors would like to thank everyone who has contributed so far to the development of these 17-cal burst disks: NASA Johnson Space Center Pathways Internship Office, WSTF Hypervelocity Team, WSTF Valve Shop, WSTF Materials Technology Group, NASA Engineering Safety Center. Also, many thanks given to the Aeroballistics Range Association for sponsoring this student paper.

References

[1] Kauderer, A., & Dunbar, B. (2010, October 23). *Space debris and human spacecraft*. Retrieved from: http://www.nasa.gov/mission_pages/station/news/orbital_debris.html

[2] Berggren , R. E., & Reynolds , R. M. NASA, Ames Research Center. (n.d.). *The light-gas-gun model launcher*, p 35,49,50. Retrieved from website: http://ntrs.nasa.gov/archive/nasa/casi.ntrs.nasa.gov/19710004103_1971004103.pdf

[3] Montgomery, D. (2012). *Design and analysis of experiments*. (8th ed.). Hoboken, NJ: John Wiley & Sons, Inc.

[4] StatSoft, Inc. (2012). *Designing an Experiment, Power Analysis***.** Electronic Statistics Textbook. Tulsa, OK: StatSoft. Retrieved from website: http://www.statsoft.com/textbook/power-analysis/.

[5] Box , M. J., & Draper, N. R. (1971). Factorial designs, the [x’x] criterion and some related matters. *Technometrics, Vol. 13*(NO.4), Retrieved from website: http://www.jstor.org/discover/10.2307/1266950?uid=3739520&uid=2&uid=4&uid=3739256&sid=21101010204843

[6] B.A. Miller, Overload Failures, *Failure Analysis and Prevention*, Vol 11, *ASM Handbook*, ASM International, 2002, p 671–699.

[7] B.A. Miller, Overload Failures, *Failure Analysis and Prevention*, Vol 11, *ASM Handbook*, ASM International, 2002, p 671–699.

[8] D. Chavez, C. Keddy, J. H. Kerr, D. Henderson, *Study of Two Stage Light Gas Gun Petal Valve Burst Pressures*, NASA Johnson Space Center - HITF and White Sands Test Facility, Presented at the 51th Aeroballistic Range Association Meeting, Madrid, PUM, 2000.

[9] Deforge, D. J. (1993). *Performance of the ubc two-stage light-gas gun*. (Master's thesis, University of British Columbia, Vancouver, Canada)Retrieved from: https://circle.ubc.ca/bitstream/handle/2429/1668/ubc_1993_fall_deforge_david.pdf?sequence=1

[10] D.T. Berry, R. Subramanian, C. Persad, A. Yeoh. *Some Observations and Experiments with Light Gas Gun Burst Diaphragms, Preliminary Result*, Institute for Advanced Technology, University of Texas at Austin, Presented at the 45th Meeting, Huntsville, AEDC, 1994.

DESIGN AND CHARACTERIZATION OF THIN STAINLESS STEEL BURST DISKS FOR INCREASING TWO-STAGE LIGHT GAS LAUNCHER EFFICIENCY

J. Tylka, K. Johnson, D. Henderson and K. Rodriguez

63rd Aeroballistics Range Association Conference 2012

Royal Military Academy

Brussels, Belgium

September 30th-October 5th, 2012

WSTF 17-cal Launcher

WSTF 17-cal Launcher

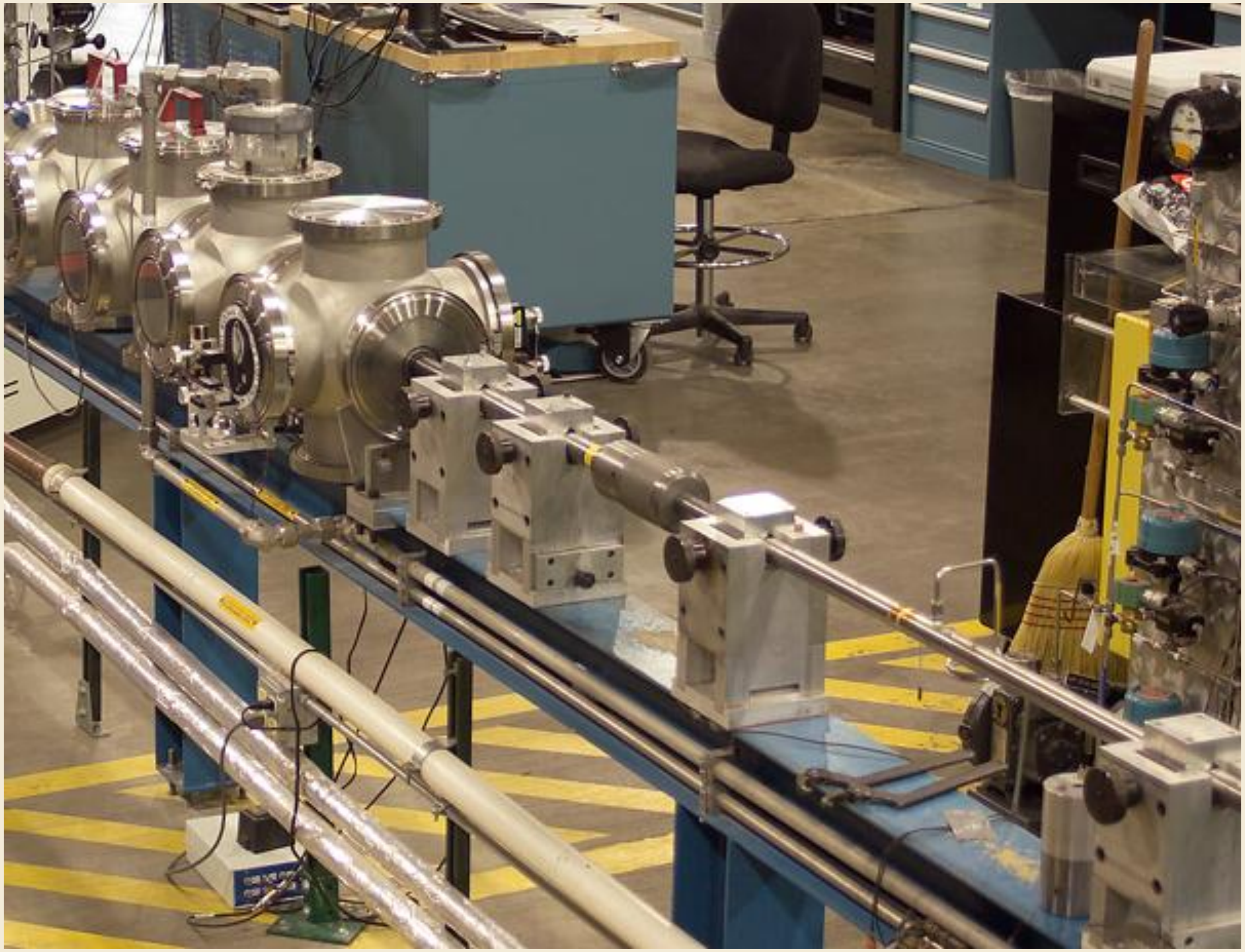

WSTF 17-cal Launcher

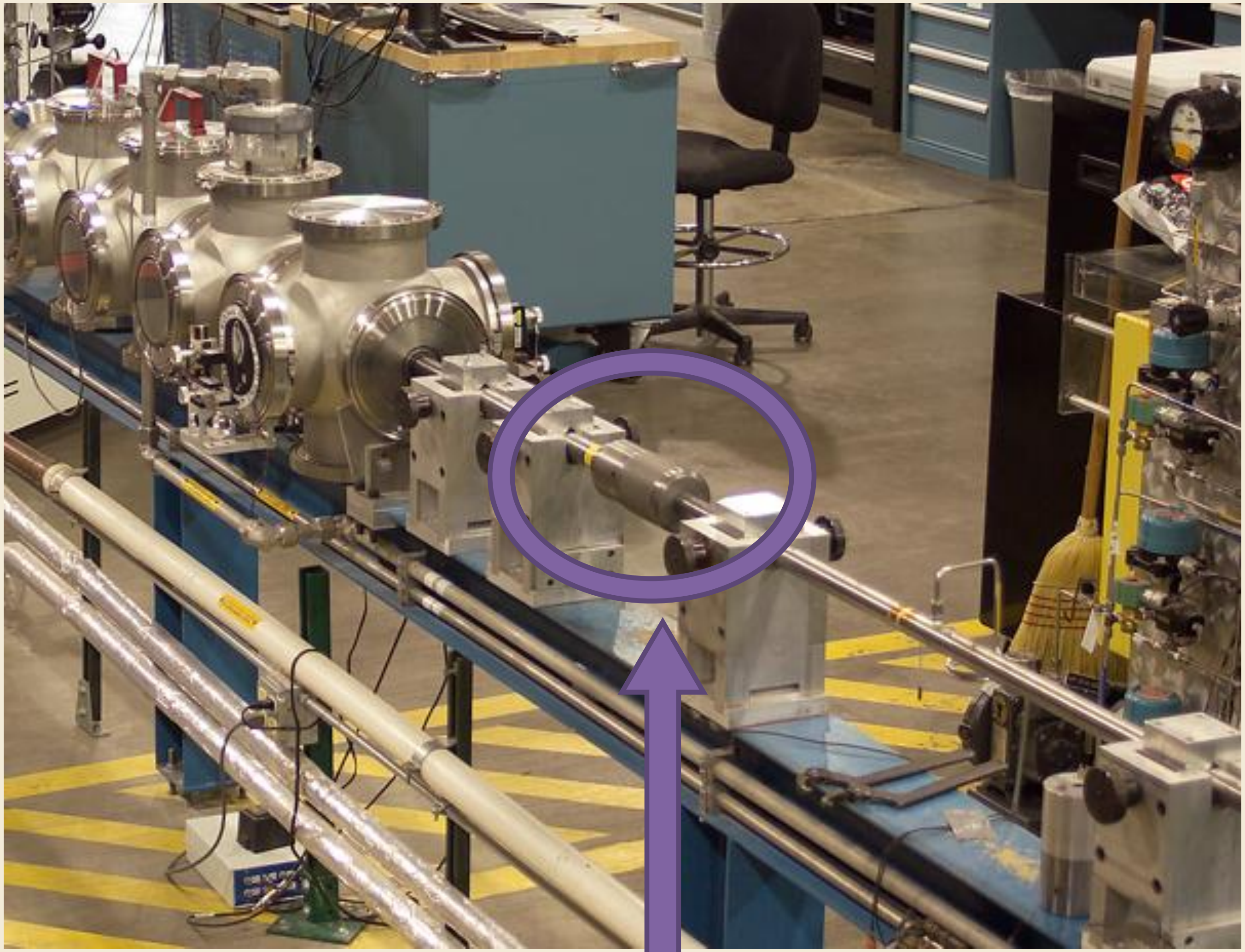

Accelerated Region (AR)

SSBD Development

- Investigate 17-cal stainless steel burst disks (SSBDs)
  - Replace aluminized Mylar
- Manufacturing Challenges
  - Disk manufacturing
  - Laser Etching
    - Fixturing
    - Heat
  - Stress concentrations
- Design Of Experiments
  - Ken Johnson NESC
- Hydrostatic Testing Valve shop
- Failure Analysis SEM

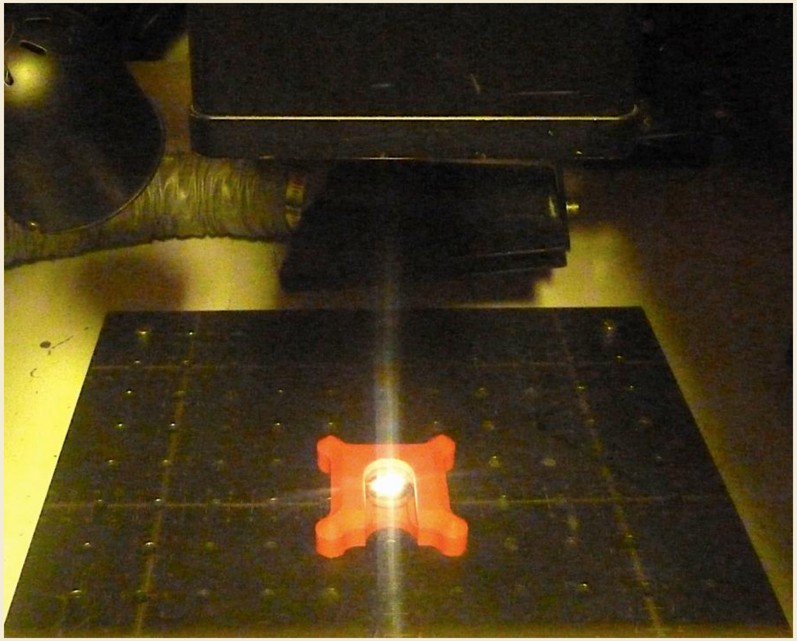

Stainless Steel Disk Manufacturing

- Wire Electric Discharge Machining (EDM)
  - Precise
  - Does not warp finished SSBD
  - Fast
  - Productive

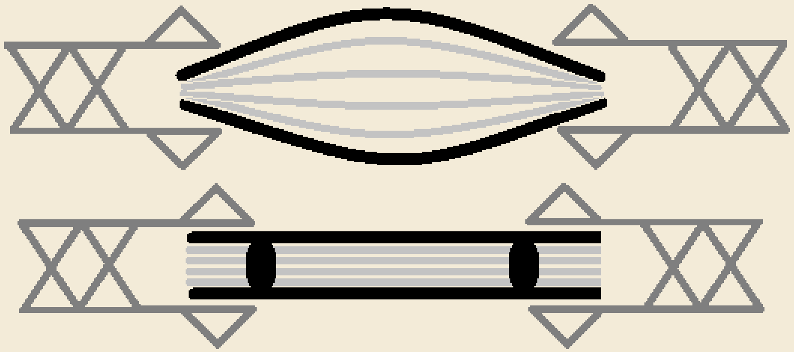

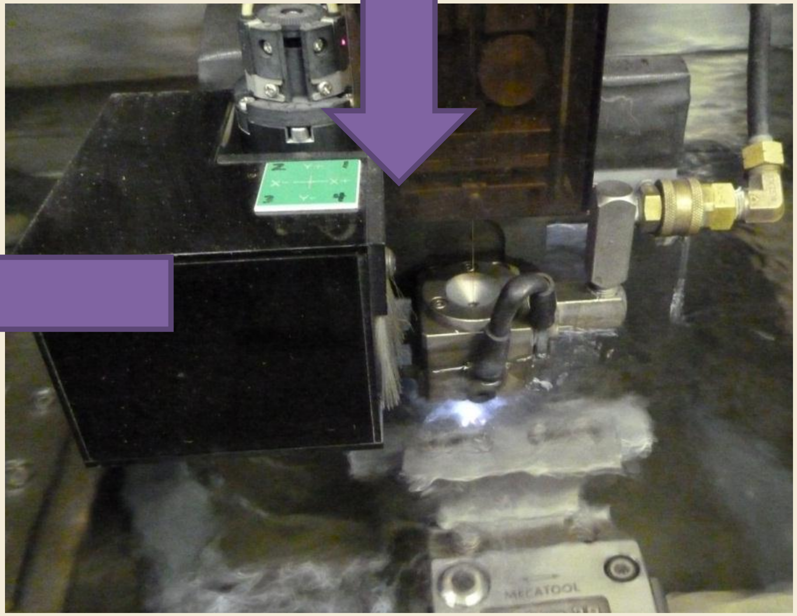

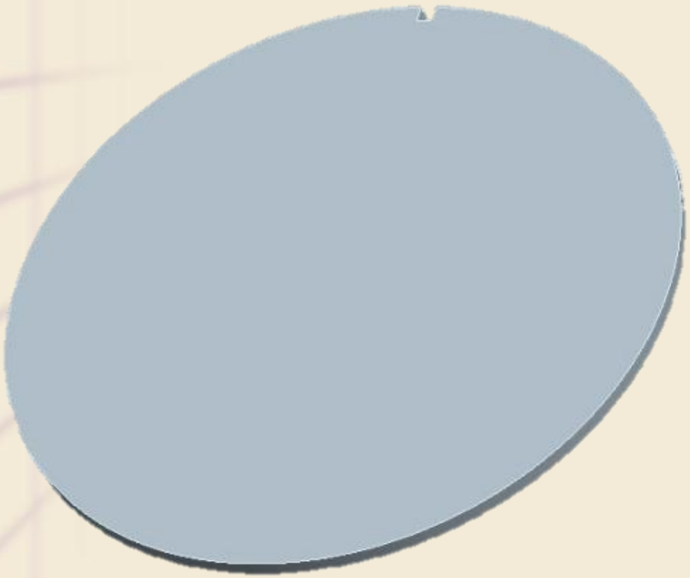

Laser Etching Fixture

- Rapid prototype
- Repeatable SSBD etching
- Index to laser
  - Dead center
  - Grain direction
    - 45° and 0°
- Final version allows for heat sink

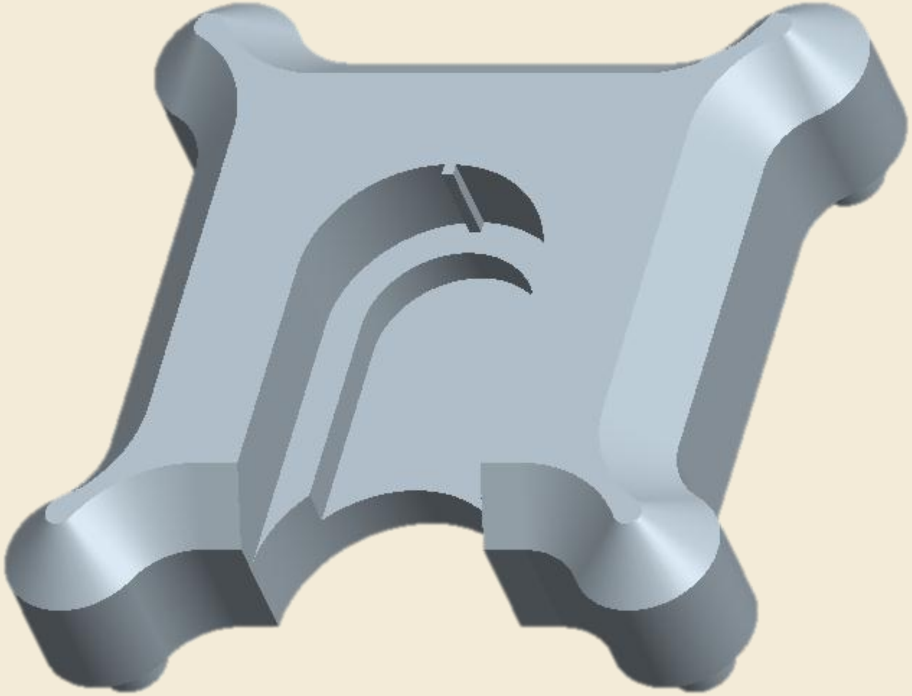

Petal Catcher

- Pros
  - Relieves stress
  - Prevents disk punch out
    - Cleaner shot result
  - Protects flow from petal action
  - Protects barrel
  - Simplifies barrel manufacturing

- Cons
  - Requires modified AR
  - Increases unsupported burst disk area
    - Decreases burst pressure
    - More debris causing potential
  - Complicates sealing
  - Increases consumables

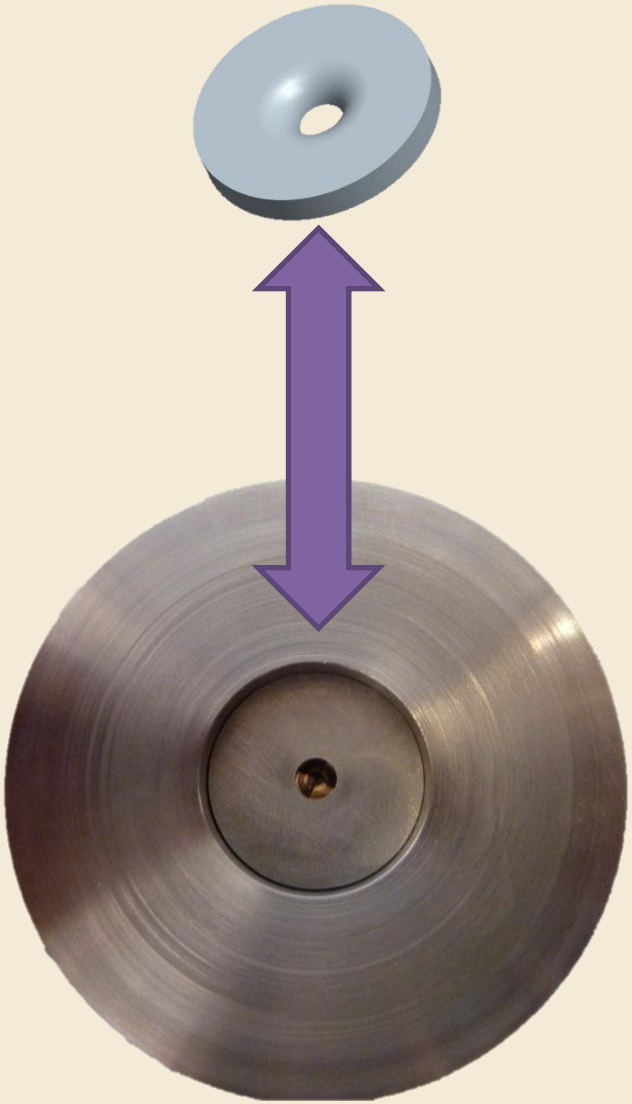

Design Of Experiments

- Statement of Problem
  - Develop process for making petal valves
    - 17-cal launcher
  - Holds on to its pieces
  - Consistently break at a designated pressure
    - Hydrostatic pressure
  - Minimum variability

- Variables
  - Stress Concentration
  - Thickness
  - Laser Runs
  - Grain direction
  - Heat Sink
  - Hardness

- Responses
  - Burst Pressure
  - Appearance of fracture
  - Fragmentation
  - Micro hardness

Experimental Matrix

Run Order	Block	Thickness	Laser Runs	Grain Direction	Heat Sink	Hardness	Burst Pressure	Failure Mode
1	NT	0.007	43	45	Without	Annealed	3236.4	ETCH
2	NT	0.02	251	0	With	Annealed	23800	ETCH
3	NT	0.015	242	0	With	Annealed	8018.2	ETCH
4	NT	0.015	46	0	With	Annealed	21545.5	ETCH
5	NT	0.02	800	45	Without	Annealed	10109.1	BURN
6	NT	0.02	93	45	With	Annealed	27436.4	ETCH
7	NT	0.015	125	0	With	Annealed	12218.2	Etch
8	NT	0.007	5	45	With	Annealed	13472.7	PUNCH
9	NT	0.007	26	0	Without	Annealed	6181.8	ETCH
10	NT	0.015	46	0	With	Annealed	20054.5	ETCH
11	NT	0.02	800	45	With	Annealed	10054.5	BURN

- 107 hydrostatic bursts preformed

Hydrostatic Burst Testing

- 1379 kPa per second (200 psi/s)
- Fixture
  - AR
  - AR Shackle
  - High Pressure Adaptor

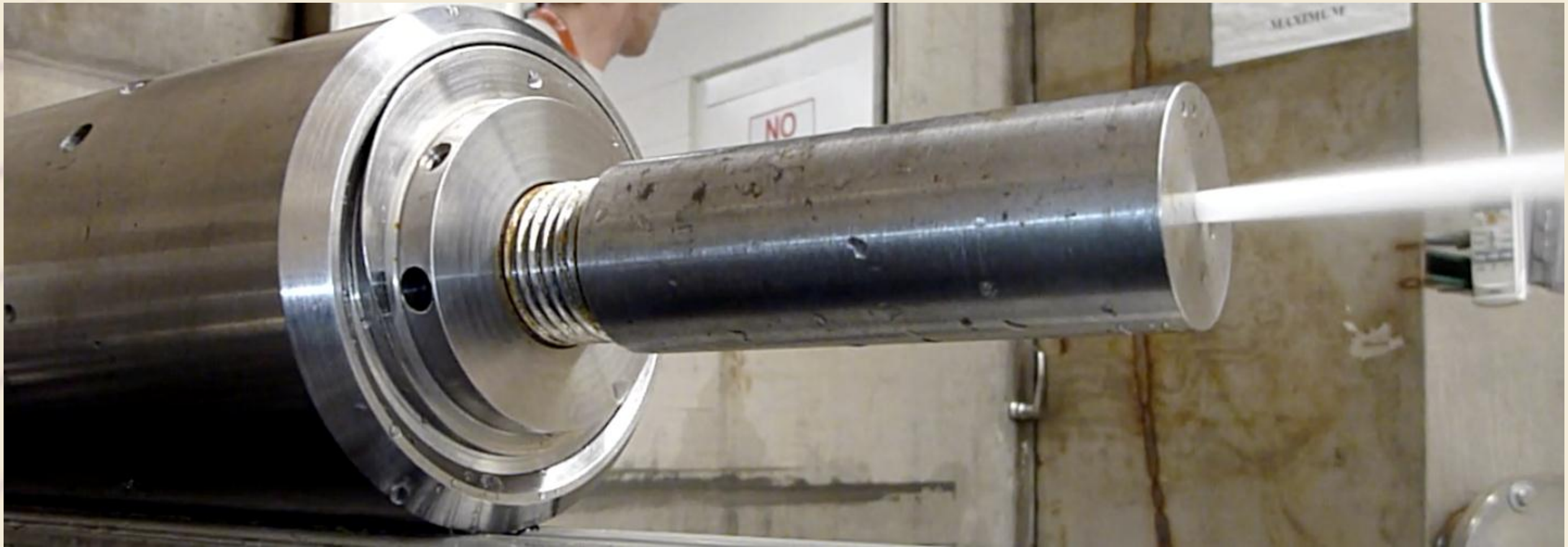

Results Of Experiments

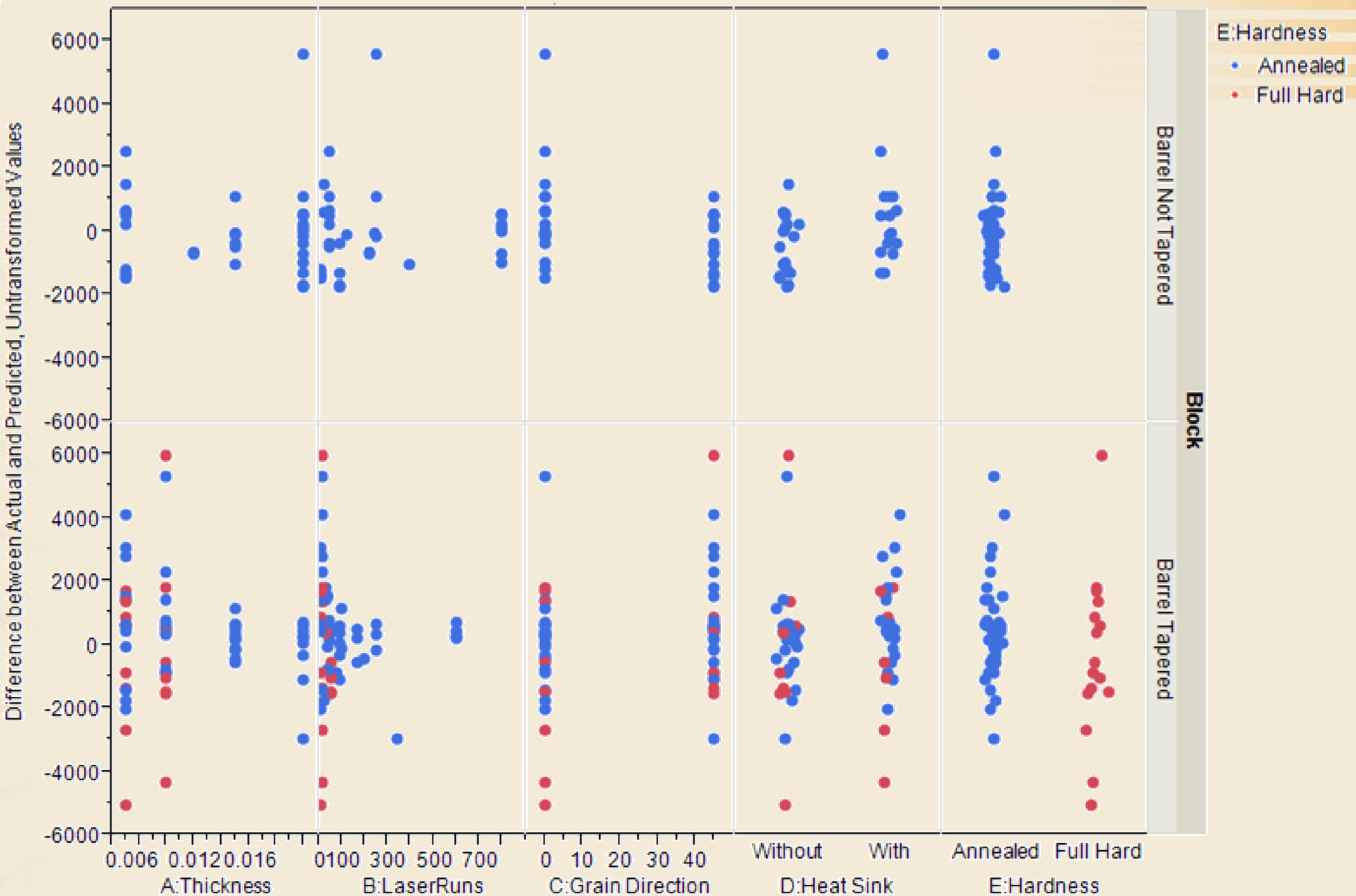

- Non-driving factors
  - Grain Direction
  - Heat Sink
  - Hardness
- Driving Factors
  - Laser runs
  - Material thickness

Tapered Barrel Model

- Modeling for tapered barrel

- $Burst\ Pressure =$
  $[104.30 + 8111.3 * Thickness - 176360(Thickness - 0.01268)^2 - 32.064 * \log_e(Laser\ Runs)]^2$

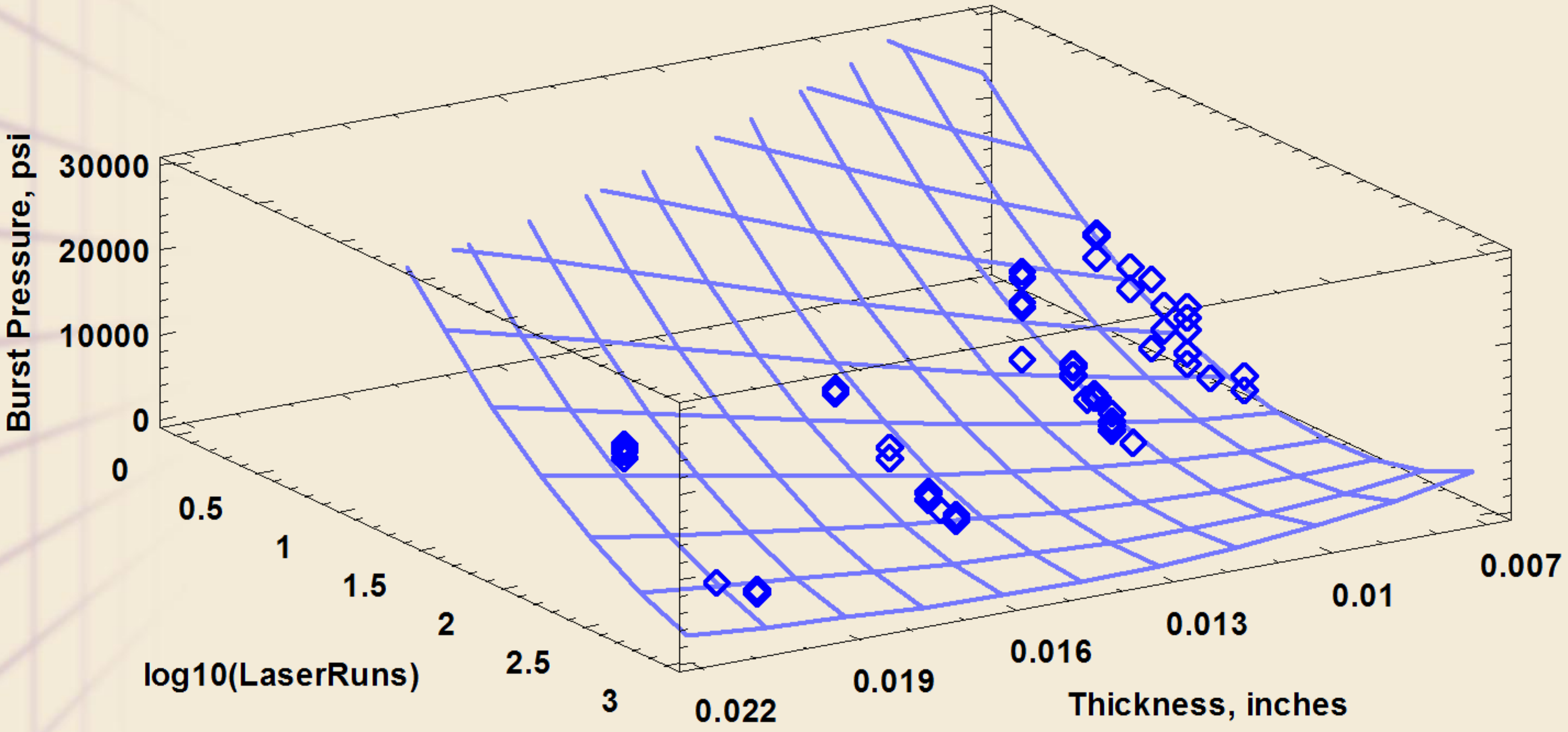

Tapered Barrel Model

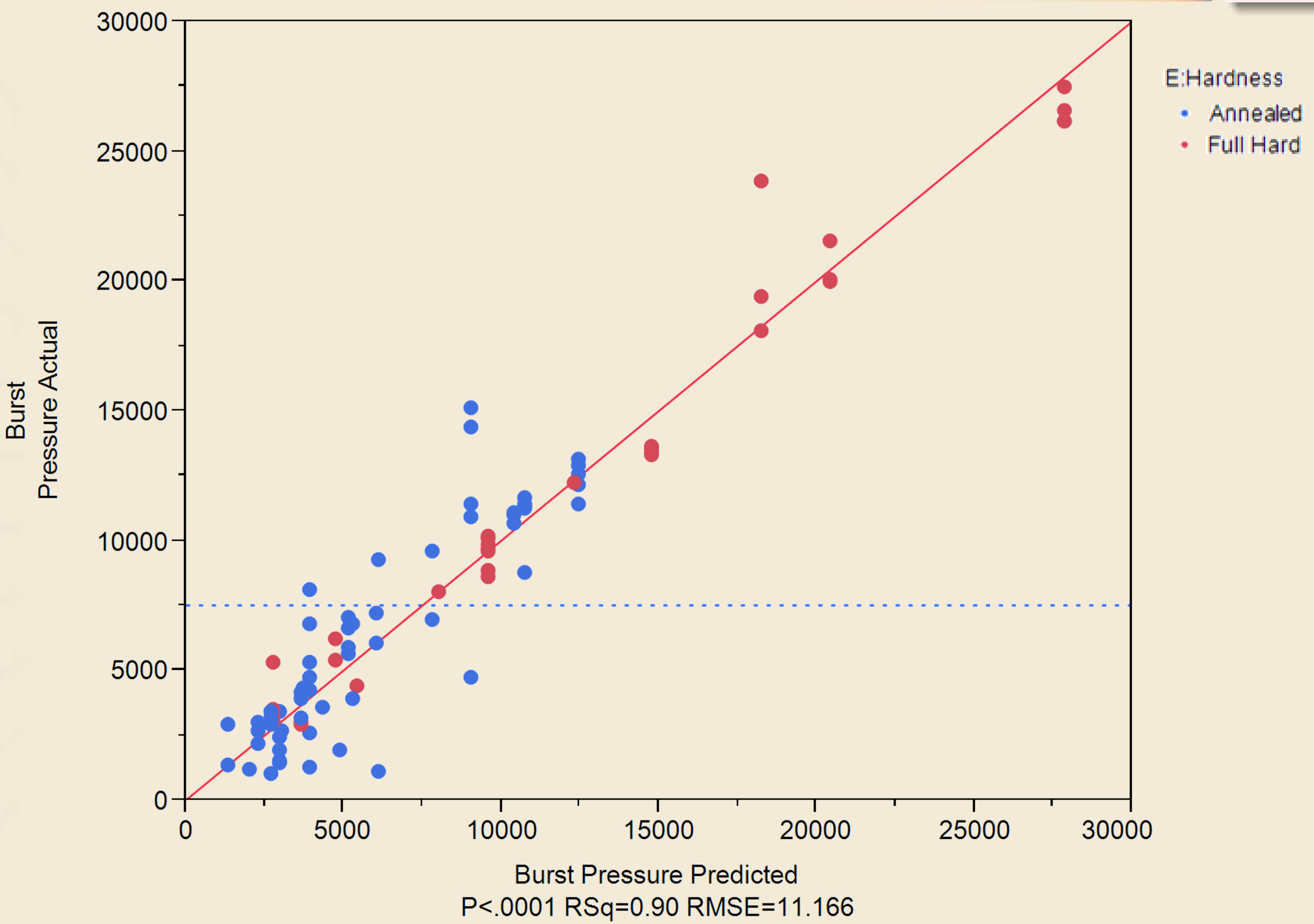

Model Comparison

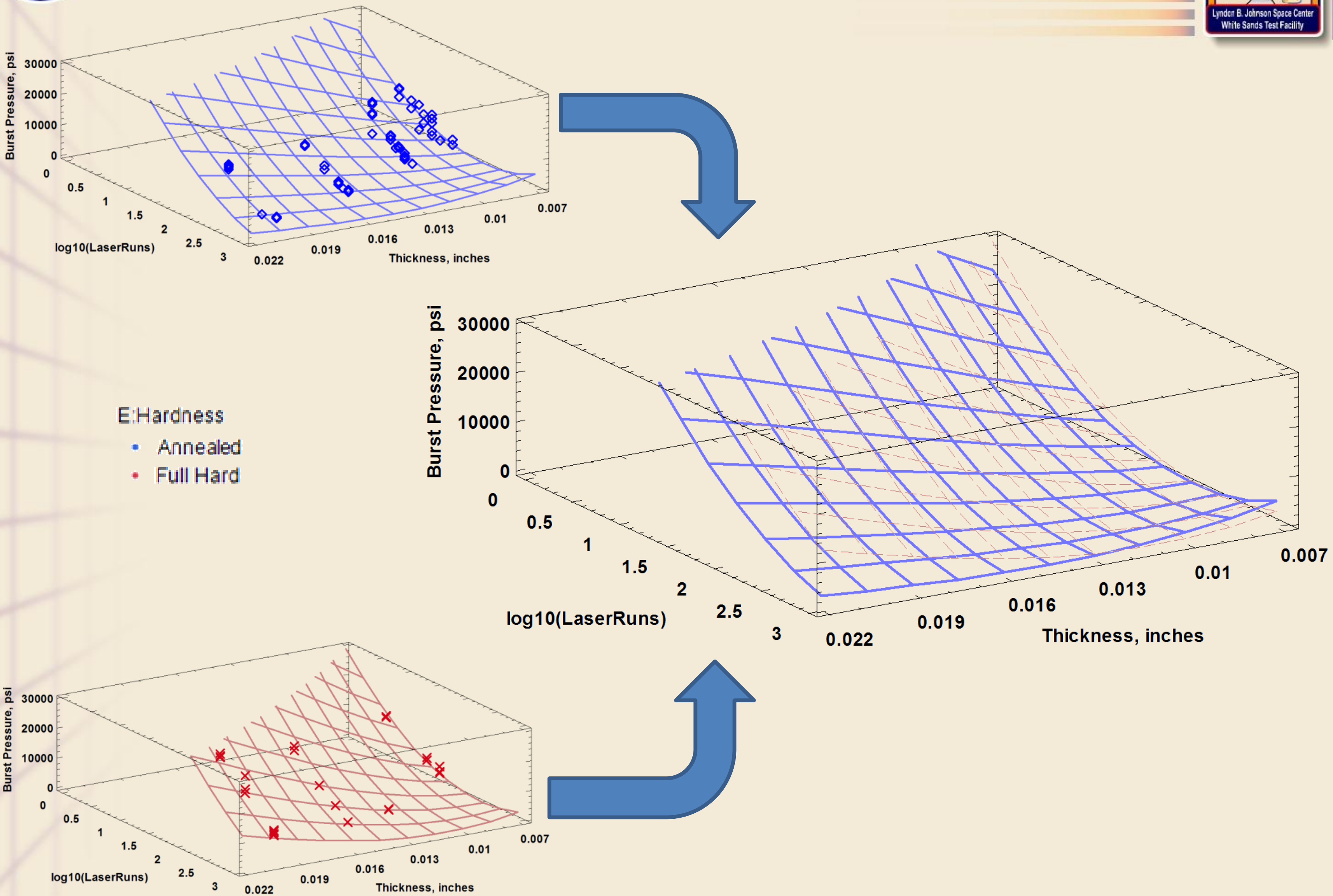

Scanning EM

- Localized fracture along laser etching
- Ductile overload failure
  - Transgranular microvoid coalescence
  - Mixed tensile and shear modes
  - Expected from austenitic stainless steel
- Non-brittle failure
  - Non-fragmenting rupture
- Gas erosion
- Manufacturing anomaly
  - Non-penetrating periodic feature

[1.] http://en.wikipedia.org/wiki/File:SEM_chamber1.JPG

Lyndon B. Johnson Space Center
White Sands Test Facility

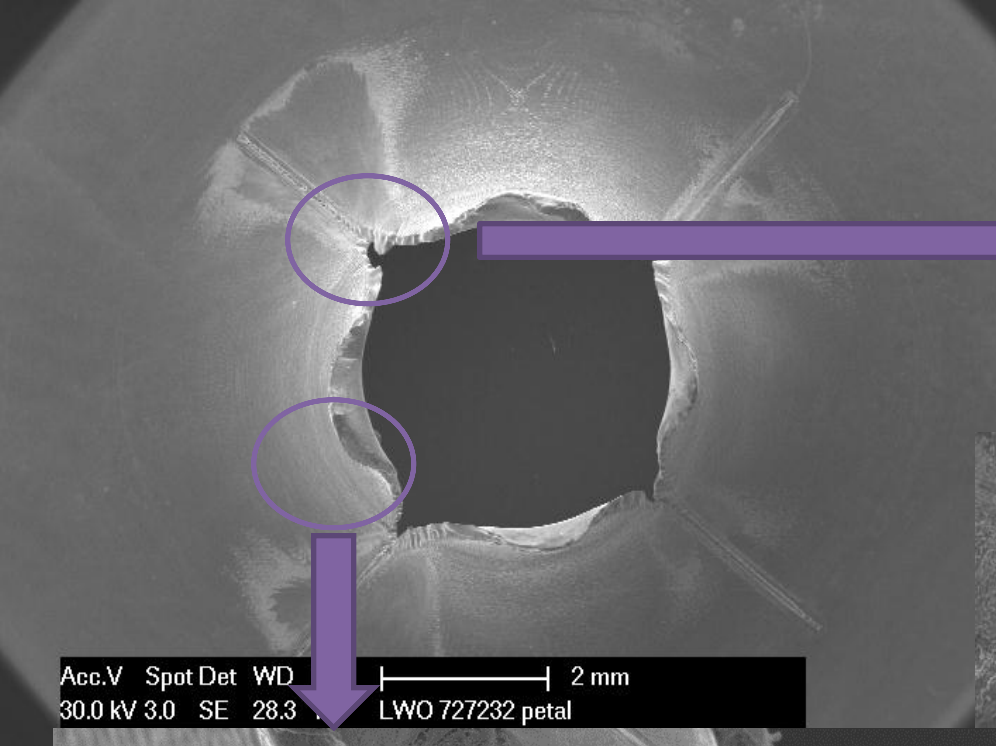

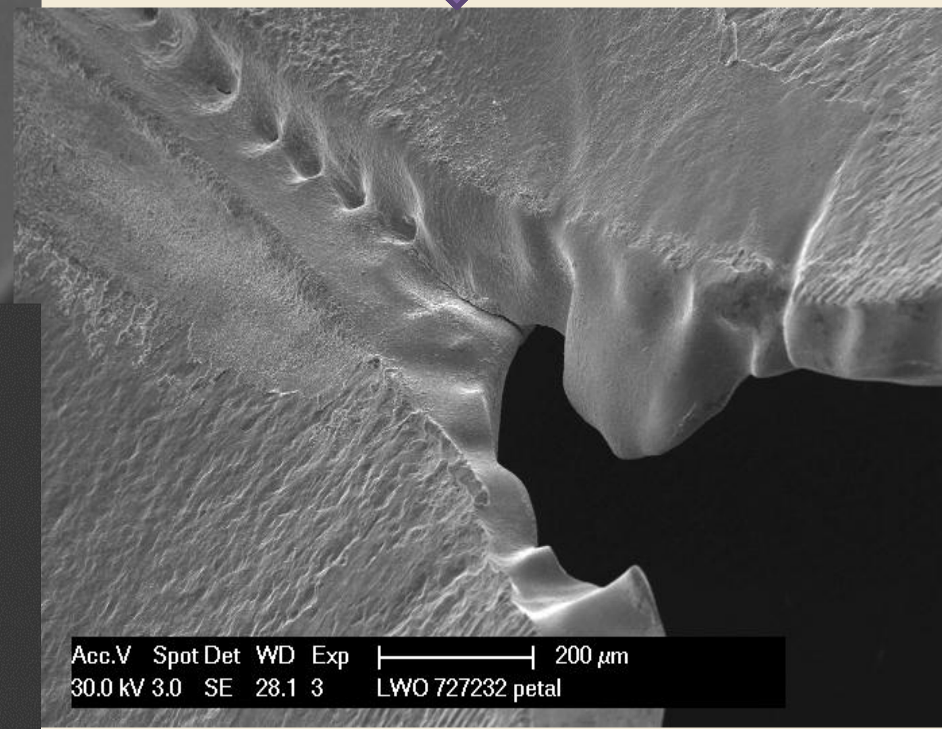

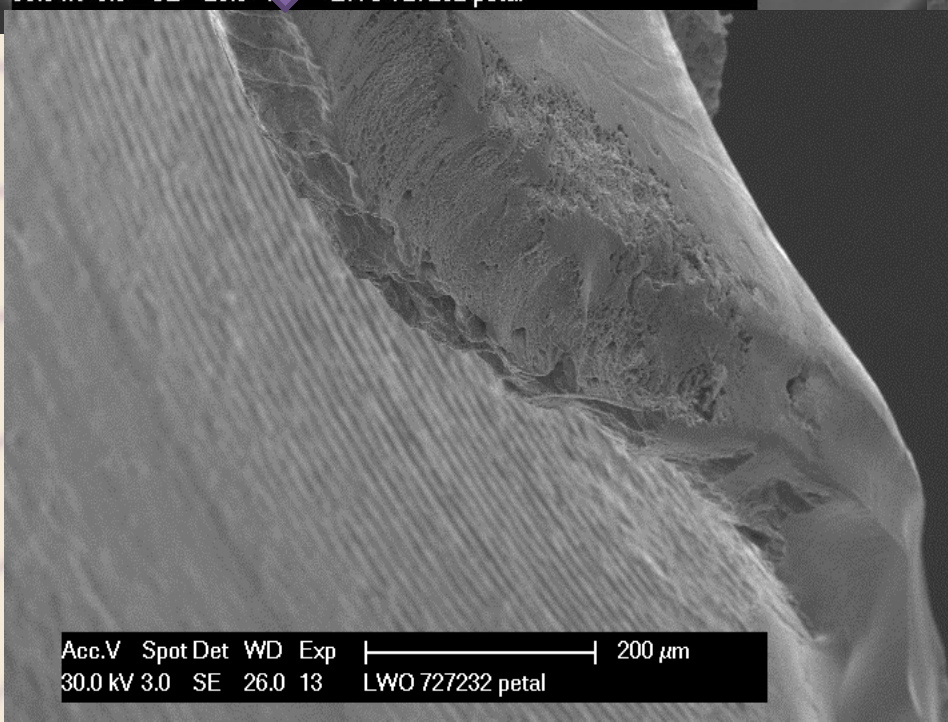

Lyndon B. Johnson Space Center
White Sands Test Facility

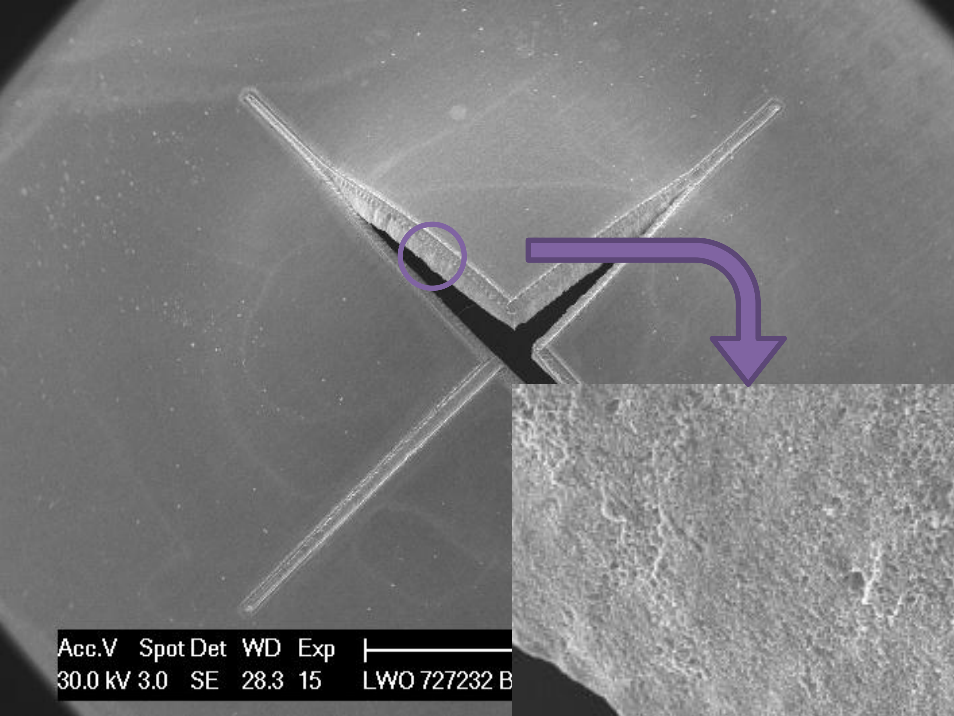

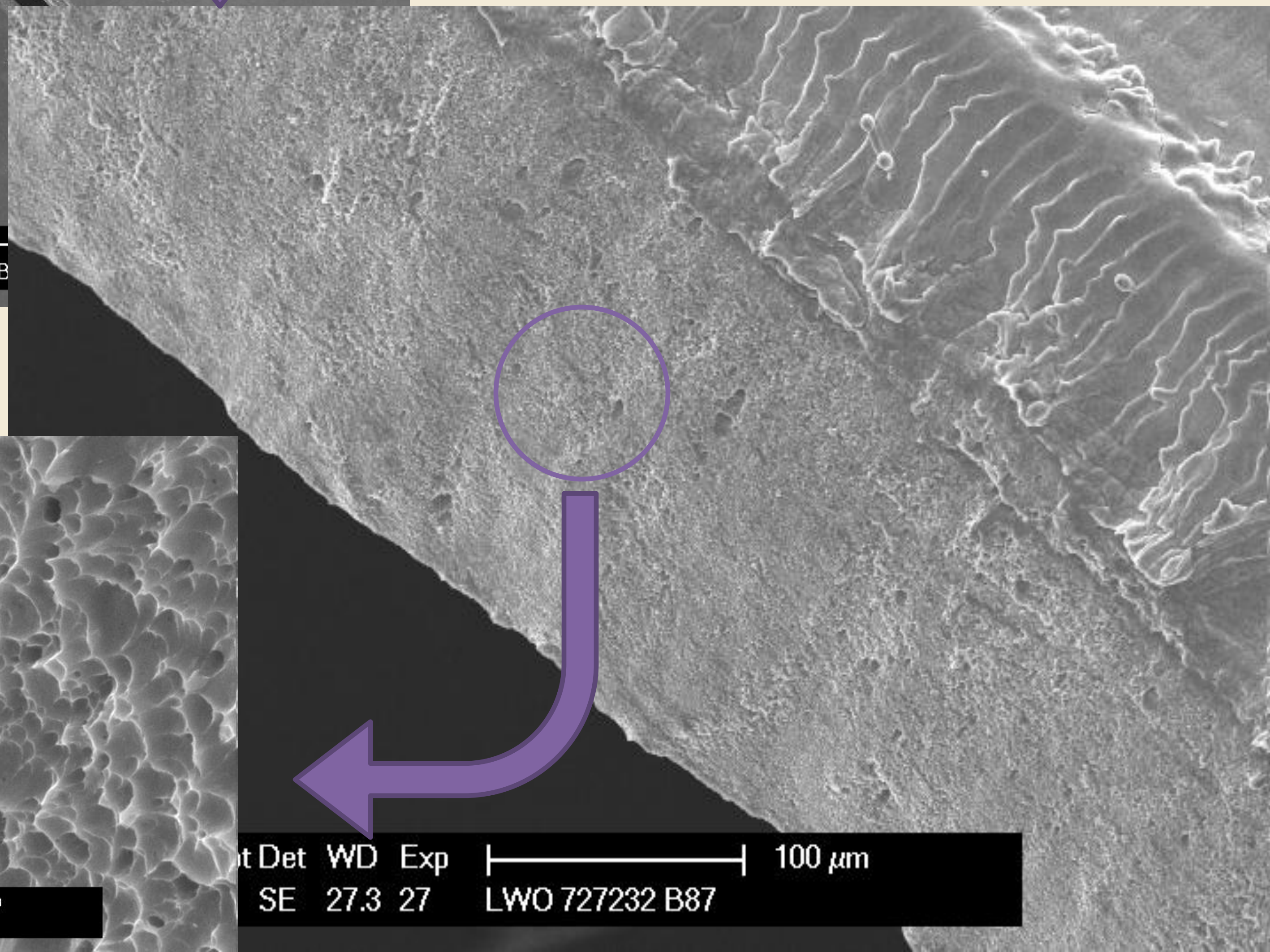

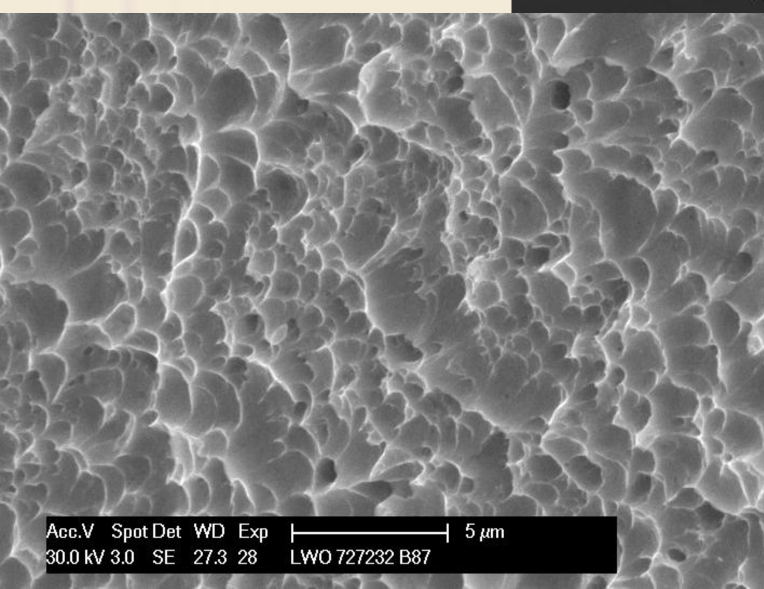


Acc.V Spot Det WD Exp
200 µm
30.0 kV 3.0 SE 28.9 35
LWO 727232 B87

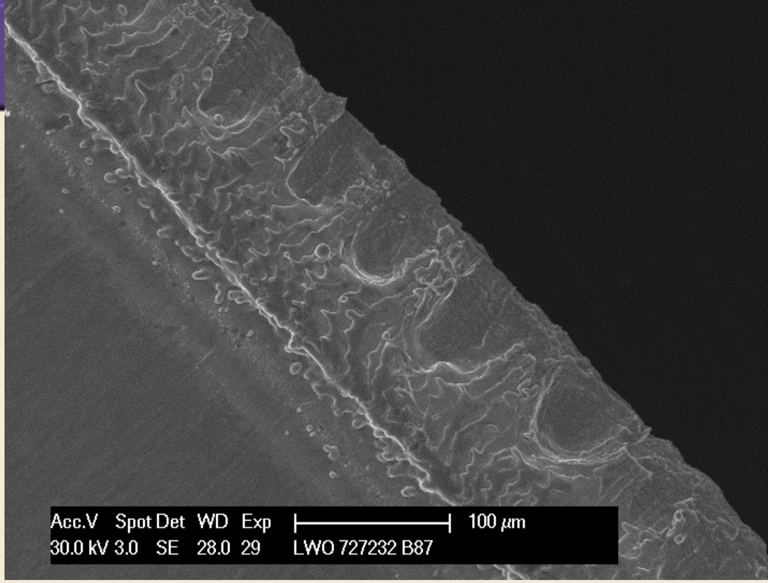
Acc.V Spot Det WD Exp
100 µm
30.0 kV 3.0 SE 28.0 29
LWO 727232 B87

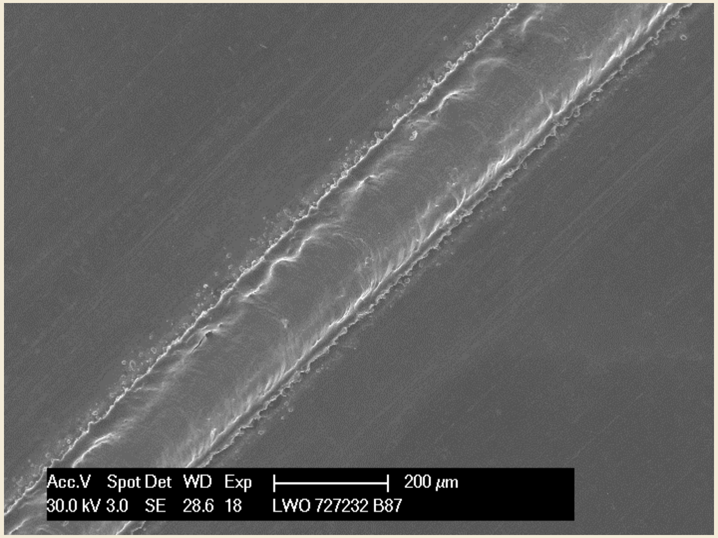
Acc.V Spot Det WD Exp
200 µm
30.0 kV 3.0 SE 28.6 18
LWO 727232 B87

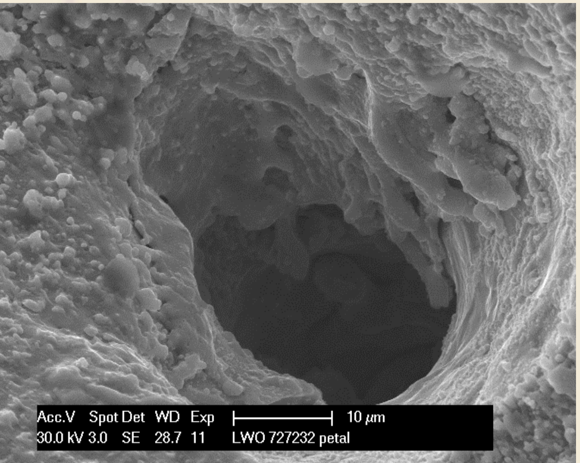
Acc.V Spot Det WD Exp
10 µm
30.0 kV 3.0 SE 28.7 11
LWO 727232 petal

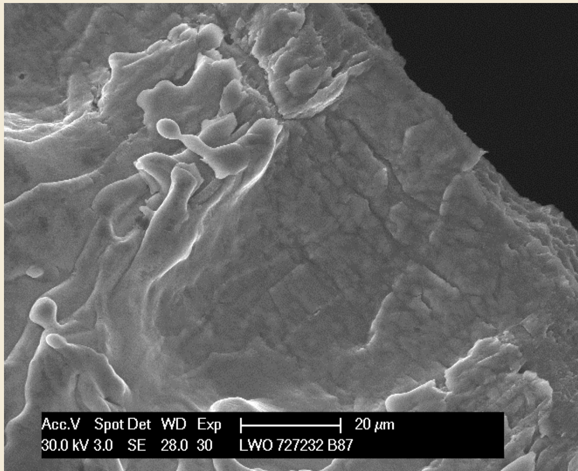
Acc.V Spot Det WD Exp
20 µm
30.0 kV 3.0 SE 28.0 30
LWO 727232 B87

Future Work

- Investigate different:
  - Laser setting
  - Disk materials
- Additional launcher testing:
  - SSBD opening time
  - Petal catcher radius
- Scaling 17-cal SSBDs:
  - Up or down for smaller and slightly larger launchers
  - Manufacturing methods up for larger launchers

Questions?

Lyndon B. Johnson Space Center
White Sands Test Facility

Thank You!

- Harold Beeson
- Karen Rodriguez
- Don Henderson
- Ken Johnson
- Darin Franzoni
- Ted Williams
- Victor Maese
- Neil Robertson
- Darren Cone
- Paul Spencer
- John Hanson
- Dennis Garcia
- Paul Mirabal
- Grant Dyer
- Art Pardo
- Miguel Maes
- Ed Alberson
- John Anderson
- Jack Cervoni
- Bill Weed

- ARA Student Outreach Program!
- Johnson Space Center Pathways Internship Program

THE END